Research in Pharmaceutical Sciences, April 2024; 19(2): 121-147
Received: 14-05-2023
Peer Reviewed: 24-06-2023
Revised: 16-07-2023
Accepted: 13-09-2023
Published: 01-04-2024

School of Pharmacy & Pharmaceutical Sciences
Isfahan University of Medical Sciences

Original Article

Determination of the anticancer activity of standardized extract of *Centella asiatica* (ECa 233) on cell growth and metastatic behavior in oral cancer cells

Suwisit Manmuan[1,*], Sukannika Tubtimsri[2], Nattaya Chaothanaphat[1], Nipatha Issaro[3], Mayuree H. Tantisira[1], and Ponwit Manmuan[4]

[1]*Division of Pharmacology and Biopharmaceutical Sciences, Faculty of Pharmaceutical Sciences, Burapha University, Chonburi, 20131, Thailand.*
[2]*Division of Pharmaceutical Technology, Faculty of Pharmaceutical Sciences, Burapha University, Chonburi, 20131, Thailand.*
[3]*Department of Community Public Health, Songkhla Community College, Songkhla, 90150, Thailand.*
[4]*Department of Intellectual Property, Ministry of Commerce, Nonthaburi, 11000, Thailand.*

Abstract

Background and purpose: The anticancer drugs used for oral cancer treatment present many disadvantages, such as low solubility, low permeability, and poor bioavailability. However, the anticancer activity of ECa 233 has not been widely studied. Therefore, the anticancer activity of ECa 233 was investigated in this study.
Experimental approach: MTT assay was carried out to determine cell viability. Characterizations of cell apoptosis were monitored using DAPI and FDA staining and Hoechst 33258 and AO staining. Confirmation of the apoptosis-induced KON cells was done using annexin V-FITC staining, and ROS generation was determined by DCFDA staining. Cell death and the cell cycle arrest activity of ECa 233 were demonstrated by a flow cytometer. The anti-migration and anti-invasion properties of ECa 233 were examined. The anti-proliferative of ECa 233 was investigated. Cellular uptake of ECa 233 was measured by TEER values. The pharmacokinetics of ECa 233 were estimated using the pkCSM web server.
Findings/Results: ECa 233 decreased the KON cell viability. Morphological analysis showed the KON cells' loss of cell stability and structure, disorganized nucleus and cytoplasm, and induced cell death. ECa 233 acted as a cell cycle arrest in the G0/G1 phase and reduced the migration and invasion ability in KON cells. TEER values significantly increased in KON cells, which decreased cell colony and multicellular spheroid formations. The pharmacokinetic profiles of the main components are of interest for future usage.
Conclusion and implication: ECa 233 can be used as an alternative therapy as well as a medicinal plant selected for sensitizing oral cancer cells to chemotherapy.

Keywords: Cell apoptosis; Cell invasion; Cell migration; Cytotoxicity; ECa 233; Oral cancer.

INTRODUCTION

Oral cancer is a type of cancer that occurs in the upper aerodigestive tract. According to the rankings, it is the sixth most common type of cancer worldwide. In particular, squamous cell carcinoma is the most common histological diagnosis accounting for approximately 90% of oral cavity cancers (OCC) (1). Tobacco and alcohol are important risk factors in cancer, with other risk factors implicated in the development of oral cancer including diet and nutrition, viruses, radiation, ethnicity, familial and genetic predisposition, oral thrush, and immunosuppression (2). Oral cancer is often preceded by a clinical premalignant phase accessible to visual inspection, which increases the opportunities for earlier detection and reduction of morbidity and mortality in oral cancer patients (3).

*Corresponding author: S. Manmuan
Tel.: +66-38390401, Fax: +66-38390400
Email: Suwisit@go.buu.ac.th

Access this article online	
	Website: http://rps.mui.ac.ir
	DOI: 10.4103/RPS.RPS_81_23

Surgical techniques, chemotherapy, and radiotherapy are constitutively the major conventional approaches applied as first-line OCC treatment protocols, which are costly and may cause adverse effects after therapy (4). Early diagnosis is crucially selected as a primary prevention and a suitable choice for therapeutic strategies. However, delay in OCC diagnosis remains a problem, resulting in high morbidity and mortality. Some patients have been identified in the advanced stages (III or IV) of OCC progression. Recurrence after primary treatment and/or metastasis are found in more than 50% of patients and the 5-year survival rate has been less than 50% in recent decades (5,6). Currently, anticancer drugs (methotrexate, 5-fluorouracil, paclitaxel, and cisplatin) are generally used alone or in conjunction with chemotherapy for oral cancer management (7). In addition, low solubility, permeability, and poor bioavailability after administration in the body are limitations for oral cancer treatment. Therefore, the search for natural products or medicinal plants to improve the efficacy of concurrent drug chemotherapy needs to be explored (8). Natural products have been shown to provide bioactive components with pharmacological activities that are well-documented in reports. These activities are associated with numerous bioactive molecules and minimal toxicity and have been extensively explored for their anticancer activity for more than a half-century (9-11).

Estrogen receptors (ERs) are classified into ERα and ERβ as nuclear receptors, which function as the transcription factors that induce the expression of genes involved in the regulation of cancer cell growth and survival. The phosphorylation and conformational changes in these receptors lead to the dissociation of heat shock proteins and processes of receptor dimerization, nuclear translocation, and binding to estrogen-responsive elements found at the promoter sites of estrogen-responsive genes. By binding to estrogen-responsive elements, the ERs catalyze the entry of coactivators or corepressors and combine them into complexes, thereby regulating the transcription process. The transcription of estrogen-responsive genes and the regulation of various physiological processes within the body physiologically facilitate DNA binding, and ligand-activated ERs can act as coactivators that regulate gene transcription by binding to transcription factors such as activating protein 1 and specificity protein 1. In addition, activation of ERs by intracellular signaling can occur in the absence of a ligand (12-14).

Previous research has shown the role of ERs in regulating hormone-regulated cancers, such as breast, prostate, ovarian, and endometrial cancers. The incidence of ERs in oral squamous cell carcinoma (OSCC) is not well understood, and the exact pathogenesis of the disease is unknown. However, in previous studies, ERα and ERβ expression has been found in OSCC tumors and cell lines, where tamoxifen therapy plays a key role in specific tumor suppression and inhibits the proliferation of cancer cells (15,16). Additionally, expression of ERα and ERβ can be found in head and neck squamous cell carcinoma tumors, but the cellular role of ERα is greater than that of ERβ in tumor lesions, predominantly in adjacent mucosa in patients with ERα. ERα-expressed tumors showed reduced cancer survival compared to cancer patients with less ERα expression, which demonstrated that head and neck squamous cell carcinoma cells overexpressed ERα, which is related to the development and growth of oral cancer (17). However, the activation of ERα and the regulatory mechanism in OSCC cells are not known (18). In this study, cancer cell motility and proliferation induction were tested using estrogen (β-estradiol) because it was expected that the cancer cells used in the study, KON cells, likely expressed the ERs inside. The expression of ERs in these cancer cells has not been reported before, from which the research team hypothesized that it is likely that the ERs are expressed in the nucleus of KON cells. Therefore, as a study to measure the response of oral cancer cells to estrogen, the data of the present study will provide a better understanding of the effects of estrogen on the habitually of KON cells concerning migration and invasion capacity, which is beneficial for drug selection in anti-hormonal agents to eradicate oral cancer cells.

Centella asiatica (ECa 233) has long been widely used as traditional herbal medicine in

Thailand and Southeast Asia (19). It possesses the major bio-composition of madecassoside and asiaticoside, characterized as a white to off-white powder and a ratio of madecassoside to asiaticoside of 1.5 ± 0.5:1 (20,21). This plant has been reported to have various pharmacological properties and has been used for its asthma, ulcer, eczema, and wound healing effects, as well as memory and learning enhancement and anxiety relief, which can contribute to a deep state of relaxation and/or mental calmness throughout meditation practices (22-26). ECa 233 also acts an as inhibitor in the lipopolysaccharide-stimulated production of inflammatory mediators in keratinocyte HaCaT cells by suppressing ERK1/2 and nuclear factor kappa B pathways, which may be related to the inhibition of reactive oxygen species (ROS) production (27). Multiple oral dosing of ECa 233 at 100 mg/kg/day for 7 days in rats has been identified. The physical appearance and blood biochemical parameters of the rats were not significantly altered after treatment with ECa 233 for 7 days. The maximum plasma concentration and area under the curve of madecassoside and asiaticoside were reduced by 70-80% in one day. Moreover, triterpenoid glycosides were extensively distributed and sustainably accumulated in the body, then typically excreted in feces (28,29).

However, the anticancer activity of ECa 233 has not been widely studied. Thus, we investigated the anticancer activity of ECa 233 toward inhibition of cell growth in KON oral cancer cells and also determined the anti-migratory ability and invasion activity under normal conditions and β-estradiol (E_2)-induced cell migration and invasion. The possible underlying mechanism associated with cells undergoing apoptosis and the effects of ECa 233 on the KON cell cycle were also evaluated. The safety profile of ECa 233 was investigated using MRC-5 normal fibroblast cells. Furthermore, this study provided the details of the anticancer activity of ECa 233 and the mechanism of cell death elicited by ECa 233, which is an additional beneficial use of ECa 233 as a new therapeutic strategy to destroy oral cancer.

MATERIALS AND METHODS

Chemicals

3-(4,5-Dimethylthiazol-2-yl)-2,5-diphenyltetrazolium bromide (MTT; AMRESCO, USA), annexin V-fluorescein isothiocyanate (FITC) apoptosis detection kit (BD Biosciences, San Diego, CA, USA), PrestoBlue™ Cell Viability Reagent (Thermo Fisher Scientific, Rockford, IL, USA), Dulbecco's modified eagle medium (DMEM), fetal bovine serum (FBS), L-glutamine, penicillin/streptomycin, 0.25% trypsin-ethylenediaminetetraacetic acid (EDTA), phenol red-free improved minimum essential medium (IMEM), charcoal-stripped FBS, and non-essential amino acids were purchased from Gibco (Gaithersburg, MA, USA). Furthermore, 0.4% trypan blue (Sigma, USA), dimethyl sulfoxide (DMSO; Sigma, USA), 96-well plates (Corning, USA), 12-well plates (Corning, USA), 24-well plates (Corning, USA), T-75 cell culture flasks (Corning, USA), Fungizone® (Gibco, USA), 4',6'-Diamidine-2'-phenylindole dihydrochloride (DAPI; Sigma, USA), fluorescein diacetate (SolarBio®, China), Hoechst 33258 (SolarBio®, China), acridine orange (AO; SolarBio®, China), BD matrigel matrix (Bioscience, USA), transwell chambers (8 μm pore size; Millipore, Billerica, MA, USA), and methanol (AMRESCO, USA) were obtained.

Cell cultures and reagents

The research was performed on KON oral cancer cells and MRC-5 fibroblast cells, which were obtained from Assistant Professor Dr. Sukannika Tubtimsri, Division of Pharmaceutical Technology, Faculty of Pharmaceutical Sciences, Burapha University. All cell lines were cultured in DMEM supplemented with 10% heat-inactivated FBS, 1% penicillin and streptomycin, and amphotericin B in an incubator (Shel Lab, USA) at 37 ℃ atmosphere with 5% CO_2 in T-25 cell culture flasks.

ECa 233 standardized extract was kindly supplied by Siam Herbal Innovation Ltd. (Samut Prakan, Thailand). The total main compounds of the standardized extract were precisely quantified by liquid chromatography-

mass spectrometry (LC-MS/MS) analysis: madecassoside (46.3%) and asiaticoside (41.6%). The stock solution of ECa 233 was solubilized using absolute DMSO. The working solution was prepared at 10 mg/mL, which was diluted by a serum-free medium. The stock solution was kept away from light and frozen in a -20 ℃ refrigeration.

Cell viability analysis by MTT colorimetric assay

Cell viability was estimated by MTT colorimetric assay. KON cells were seeded at a density of 10,000 cells into a 96-well plate for 24 h. Then, the medium was replaced with ECa 233 at 0.78125, 1.5625, 3.125, 6.25, 12.5, 25, 50, 100 µg/mL for 24, 48, 72, and 96 h. Then, 10 µL of 5 mg/mL yellow MTT in phosphate-buffered saline (PBS) solution was added to each well and further incubated for 3 h. To solubilize the purple formazan crystals, 100 µL of absolute DMSO was added to each well. The plate was shaken and incubated in a dark room for 15 min. The optical density (OD) was read by a microplate reader (FLUOstar Omega, Germany) at 570 nm. The percentage of cell viability was calculated using the equation (1) provided below:

$$\text{Cell viability (\%)} = \frac{\text{OD of sample} - \text{OD of blank}}{\text{OD of control} - \text{OD of blank}} \times 100 \quad (1)$$

The percentage of cell viability was expressed as mean ± SEM. The controls were calculated to 100% cell viability for each assay. The data obtained were used to calculate the concentration of the ECa 233 required to kill 50% of the KON cells (IC_{50}).

Morphological observation

KON cells were seeded at a density of 10,000 cells/well in a 6-well plate for 24 h. On the following day, the old medium was aspirated from the six wells. Cells were treated with ECa 233 at 25, 50, 100, and 200 µg/mL for 24 h. Morphological change and cells undergoing apoptosis and death after exposure to ECa 233 were monitored by a 40× magnification objective light microscope (Olympus, Japan). Nuclear shrinkage, chromatin condensation, loss of plasma membrane integrity, and formation of apoptotic bodies were generally characteristic of programmed cell death.

Nuclear and cytoplasm analysis

KON cells were cultured at a density of 10,000 cells/well on sterile glass coverslips in a 6-well plate and treated with ECa 233 at 25, 50, 100, and 200 µg/mL for 24 h. Media was aspirated from each well. Cells were washed twice with 1× PBS solution to remove floating cells. Cells were fixed with 4% paraformaldehyde for 15 min and permeabilized with 0.2% Triton®-X-100. Cells were stained with 2.5 µg/mL DAPI (molecular probes) and 0.5% fluorescein diacetate (FDA) for 30 min in a dark room. Cells were washed with PBS, and the coverslips were sealed onto the slides. The cytomorphology of the KON cells was examined using an inverted fluorescent microscope (ECLIPSR Ts2, Nikon, Japan) at 40× objective magnification.

Morphological determination of apoptotic cells

KON cells at a density of 10,000 cells/well were grown on sterile glass coverslips in a 6-well plate for 24 h in a humidified atmosphere of 5% CO_2, 37 ℃ in an incubator. The KON cells were treated with ECa 233 at 25, 50, 100, and 200 µg/mL for 24 h. Treatment-free cells were used as the negative control of the experiment. The KON cells were washed twice with 1× PBS solution and fixed with 4% paraformaldehyde for 15 min and permeabilized with 0.2% Triton®-X-100. Cells were stained with 5 µL of Hoechst 33258 and 5 µL of acridine orange (AO) for 30 min in dark conditions. Cells were washed with PBS and the coverslips were sealed onto slides. The apoptosis of the KON cells was observed using an inverted fluorescent microscope (ELIPSR Ts2, Nikon, Japan) at 40× objective magnification.

Apoptosis determination

Loss of cell membrane structure is one of the earliest characteristic features during apoptosis. In apoptotic cells, the phospholipid phosphatidylserine is translocated from the inner to the outer leaflet of the cell membrane,

while annexin V-FITC has a high affinity to the binding sites of phospholipid phosphatidylserine and serves as a probe during apoptosis investigation. KON cells were seeded at a density of 10,000 cells/well on sterile glass coverslips in a 6-well plate. Cells were treated with ECa 233 at 25, 50, 100, and 200 µg/mL for 20 h. Fixed cells and non-fixed cells on the sterile coverslips were stained with annexin V-FITC (BD Biosciences, San Diego, CA, USA). The probe-labeled cells were further incubated for 15 min in a dark room at room temperature. The cells were washed with PBS, then the excess was probed and analyzed using an inverted fluorescent microscope (ECLIPSE Ts2, Nikon, Tokyo, Japan). The number of apoptotic cells was counted from three independent experiments.

Determination of intracellular ROS

To determine the amount of ROS in the KON cells treated with ECa 233, the DCFDA cellular reactive oxygen species detection assay kit (Abcam, UK) was utilized. In this experiment, 2', 7'-dichlorofluorescin diacetate (DCFDA) was employed to assess the hydroxyl, peroxyl, and other ROS activity within the KON cells. DCFDA can penetrate the cellular level and is deacetylated by esterases, a type of enzyme, to a nonfluorescent, which can later be oxidized by ROS and altered into a fluorescent dye DCF. The generation of green fluorescence inside KON cells is directly proportional to the amount of ROS generation, which possibly implies ROS-mediated cell death. To experiment, the KON cells were seeded at a density of 10,000 cells/well in a 6-well plate for 24 h, then treated with ECa 233 at 25, 50, 100, and 200 µg/mL for 24 h. The cells were washed with PBS buffer and stained with 25 µM DCFDA in PBS buffer for 45 min at 37 °C. The KON cells were washed twice with PBS buffer. The amount of green fluorescence inside the KON cells was captured with an inverted fluorescent microscope (ECLIPSR Ts2, Nikon, Tokyo, Japan).

Determination of cell death by propidium iodide

KON cells were grown at a density of 10,000 cells/well in a 6-well plate for 24 h and then exposed to ECa 233 at 25, 50, 100, and 200 µg/mL for 24 h. Cells were harvested by trypsin/EDTA and washed with 1× PBS twice. The cell pellets were collected by centrifugation and resuspended in 1× cold PBS solution. Cells were stained with propidium iodide (PI) for 15 min in the dark at room temperature, following the manufacturer's instructions. Cells were analyzed by a flow cytometer (CytoFLEX; Beckman Coulter, Inc.). The red fluorescence of PI was detected by the PI channel (excitation = 535 nm, emission = 615 nm).

Cell cycle analysis using flow cytometry

The cell cycle was analyzed using the CytoFLEX (Beckman Coulter, Inc.) flow cytometer. The principle of this method is analysis that is based on the amount of DNA content within cells. KON cells were seeded at a density of 10,000 cells/well in a 6-well plate overnight. KON cells were incubated with ECa 233 at 25, 50, 100, and 200 µg/mL for 24 h. The cells were trypsinized by trypsin/EDTA and fixed with absolute ethanol for 24 h and kept at 4 ℃. The cell pellets were collected by centrifugation (1000 rpm, 5 min) and resuspended in 1 mL of PBS. Subsequently, the KON cells were stained with PI for 30 min. The red fluorescence was detected by CytoFLEX (Beckman Coulter, Inc.) at the excitation wavelength of 488 nm.

Wound healing assay

To determine the anti-migration effect of ECa 233 on KON oral cancer cells using monolayer cells, the KON cells were cultured in a 6-well plate in the appropriate DMEM culture medium containing 10% FBS until cell growth to the monolayer was complete. A sterile 200 µL yellow pipette tip was utilized to generate the wound by making three scratches in the cell monolayer. After washing with PBS to remove floating cells and cell debris, cells were exposed to 25, 50, 100, and 200 µg/mL of ECa 233 for 18, 24, and 48 h. Cells were photographed and observed under an inverted microscope (Olympus, Tokyo, Japan) at different time points (0, 18, 24, and 48 h). The width of the wound scratch was measured using ImageJ software (version 1.47, NIH, USA).

Colony-forming activity assay

To determine the anti-growth activity related to the formation of large colonies of KON cells, the cells were seeded at a density of 2,500 cells/well in a 12-well plate for 24 h and then cultured in DMEM in the presence or absence of ECa 233 at 25, 50, 100, and 200 µg/mL for 24 h. The old culture medium was removed, and a fresh medium was added to the culture for a further seven days. Culture media was discarded from each well. Cells were washed with 1× PBS to remove the floating cells. Cell colony formation was fixed with acetic acid (3): methanol (7) for 15 min. Cells were stained with 0.5% crystal violet for 30 min and then captured with five random fields/wells using a 4× objective magnification inverted microscope (Olympus, Japan). The data were presented as the percentage of the colony formation.

Transwell migration assay

To determine the anti-migration ability of ECa 233 in KON cells using transwell cell culture chambers, the KON cells were re-suspended in 500 µL of serum-free medium and seeded into the upper chamber (1,000 cells/well) with the presence or absence of ECa 233 at 25, 50, 100, and 200 µg/mL for 48 h. The lower compartments of the system were filled with DMEM supplemented with 10% FBS as a chemo-attractant. Subsequently, non-migrated cells remaining on the upper surface of the upper chamber were carefully discarded using a cotton swab. The migrated cells were washed twice with PBS and fixed with ice-cold methanol for 15 min at room temperature. Migrated cells that adhered to the lower compartment of the upper chamber were stained with 500 µL of 0.5% crystal violet and randomly photographed using an inverted microscope with 10× objective magnification (Olympus, Japan) in five random fields. Each insert was counted and analyzed using NIH image software. Data were calculated according to the equation (2) provided below:

$$\text{Proportion of migrated cells (\%)} = \frac{\text{Number of cells migrated in treated cells}}{\text{Number of cells migrated in untreated cells}} \times 100 \quad (2)$$

Matrigel-coated invasion assay

The Matrigel-coated invasion assay was performed to assess the intravasation and extravasation abilities of KON cells. The BD Matrigel matrix was diluted with serum-free DMEM medium, and 30 µL of Matrigel solution was added to the upper surface of the invasion chamber, which was placed in a 24-well plate. The KON cells were trypsinized by trypsin/EDTA and resuspended with a serum-free DMEM medium. Cells (at the density of 1,500 cells/well) were pipetted into the upper chamber of the invasion chamber (pore size: 8 µM; Corning, Cambridge, MA, USA) in the presence or absence of ECa 233 (25, 50, 100, and 200 µg/mL) for 48 h. The lower chamber was filled with 500 µL DMEM supplemented with 10% FBS as a chemo-attractant. Cells that invaded the lower compartment of the invasion membrane were fixed with ice-cold methanol (AMRESCO, USA) for 15 min. Non-invading cells were wiped off the upper surface of the invasion chamber with a cotton swab. Fixed cells were stained with 0.5% crystal violet for 30 min. Upper chambers were washed with 1× PBS three times. The number of invading cells was captured with five random fields/wells using an inverted microscope at 10× objective magnification (Olympus, Japan). The data were calculated using the equation (3) provided below:

$$\text{Cell invasion (\%)} = \frac{\text{Number of cells invaded in treated cells}}{\text{Number of cells invaded in untreated cells}} \times 100 \quad (3)$$

Deprivation of the estrogenic effect from phenol red DMEM media

Before the experiments, KON cells were cultured in DMEM supplemented with 10% FBS for 3 days. Then, the growth factor of the cells cultured in DMEM supplemented with 5% FBS for 2 days was decreased. The KON cells were further weaned off the estrogenic effect from phenol red, in which one composition in DMEM media was cultured in phenol red-free DMEM media and added into a 5% charcoal-stripped FBS serum for 2 days. The KON cells that were deprived of the estrogenic effect were used in the transwell migration assay and Matrigel-coated invasion assay in the E_2-induced cell migration and invasion conditions.

Transwell migration assay in E_2-induced cell migration condition

The KON cells were re-suspended in 500 µL of phenol red-free DMEM and seeded into the upper chamber (1,000 cells/well) with the presence or absence of ECa 233 at 25, 50, 100, and 200 µg/mL for 48 h. The lower compartments of the system were filled with 500 µL phenol red-free DMEM media + 5 µg/mL of E_2 as a chemo-attractant. Subsequently, non-migrated cells remaining on the upper surface of the upper chamber were carefully discarded using a cotton swab. The migrated cells were washed twice with PBS and fixed with ice-cold methanol for 15 min at room temperature. Migrated cells that adhered to the lower compartment of the upper chamber were stained with 500 µL of 0.5% crystal violet and randomly photographed using an inverted microscope with 10× objective magnification (Olympus, Japan) in five random fields. Each insert was counted and analyzed using NIH image software. Data were presented as % proportion of migrated cells in E_2-induced cell migration condition calculated using the following equation (4)

$$\text{Cell migration (\%)} = \frac{\text{Number of cells migrated in treated cells}}{\text{Number of cells migrated in untreated cells}} \times 100 \quad (4)$$

Matrigel-coated invasion assay in E_2-induced cell invasion condition

The BD Matrigel matrix was diluted with phenol red-free DMEM media to prepare the stock solution. Thirty µL of the Matrigel working solution was added to the upper surface of the invasion chamber, which was inserted in a 24-well plate. The KON cells were trypsinized by trypsin/EDTA and resuspended with the phenol red-free DMEM medium. Cells (at the density of 1,500 cells/well) were pipetted into the upper chamber of the invasion chamber (pore size: 8 µM; Corning, Cambridge, MA, USA) in the presence or absence of ECa 233 (25, 50, 100, and 200 µg/mL) for 48 h. The lower chamber was filled with 500 µL phenol red-free DMEM medium + 5 µg/mL of E_2 as a chemo-attractant. Invading cells that invaded the lower compartment of the invasion membrane were fixed with ice-cold methanol (AMRESCO, USA) for 15 min. The non-invading cells were wiped off the upper surface of the invasion chamber with a cotton swab. Fixed cells were stained with 0.5% crystal violet for 30 min. The upper chambers were washed with 1× PBS for 3 times. The number of invading cells was captured with five random fields/wells using an inverted microscope at 10× objective magnification (Olympus, Japan). The data were expressed as the percentage of cell invasion in the E_2-induced cell invasion condition using the equation (5)

$$\text{Cell invasion (\%)} = \frac{\text{Number of cells invaded in treated cells}}{\text{Number of cells invaded in untreated cells}} \times 100 \quad (5)$$

Transepithelial electrical resistance measurements

transepithelial electrical resistance (TEER) values are a quantitative determinant of the barrier integrity, which is responsible for the cellular uptake of ECa 233 of a monolayer cell. KON cells (10,000 cells/well) were cultured in a 6-well plate for 24 h. Cells were treated with ECa 233 which was present in DMEM medium at 25, 50, 100, and 200 µg/mL for 24 h. A Millicell® ERS-2 Voltohmmeter (Merck KGaA, Darmstadt, Germany) was used to determine the TEER values, which were presented as the average of ohm from three independent experiments.

Multi-cellular spheroid formation assay

KON cells at a density of 10,000 cells/well were seeded in a 96-well round bottom plate supplemented with DMEM containing 10% FBS, 1% L-glutamine, and 1% penicillin/streptomycin for 4 days. The KON oral cancer spheroids were tested to evaluate their sensitivity to 25, 50, 100, and 200 µg/mL of ECa 233 for 24 h. To determine the cell viability of KON cells, the spheroid formations were incubated with 10 µL of PrestoBlue™ reagent for 15 min. After the incubation period, the fluorescence intensity of resorufin was monitored with a fluorescence microplate reader (FLUOstar Omega, Germany) at 570 nm. The percentage of cell viability was obtained from the comparative fluorescence intensity of treated cells to non-treated cells. Spheroid formations were photographed with an inverted fluorescent microscope (ECLIPSR Ts2, Nikon, Tokyo, Japan) at 40× objective magnification.

Toxicity assessment

To assess the acute toxicity and sub-chronic toxicity of ECa 233 on the cell viability of normal cells, MRC-5 normal fibroblast cells were cultured in a 96-well plate at a density of 10,000 cells/well in DMEM media. The cells were exposed to ECa 233 at 0.78125, 1.5625, 3.125, 6.25, 12.5, 25, 50, and 100 µg/mL for 8, 22, and 30 h. Cell viability was determined using the MTT cell viability assay. The absorbance values were determined by a microplate reader (FLUOstar Omega, Germany) at 570 nm. The percentage of cell viability was evaluated and a graph was plotted for cell viability using GraphPad Prism software Ver. 8.0 (San Diego, California).

In silico pharmacokinetic properties of madecassoside and asiaticoside prediction

The pharmacokinetic properties (absorption, distribution, metabolism, excretion) of madecassoside and asiaticoside were estimated by using the pkCSM web server to illustrate the % of human intestinal absorption and the steady-state volume of distribution of madecassoside and asiaticoside was predicted. The cytochrome P-450 (CYP) enzyme inhibition (CYP2D6, CYP3A4, CYP1A2, CYP2C19, CYP2C9, CYP2D6, and CYP3A4) was used to predict the metabolism of madecassoside and asiaticoside. Excretion after administration was predicted based on total clearance and renal organic cationic transporter 2 (OCT2) substrate.

Statistical analysis

Data were collected from at least three separate experiments and presented as mean ± SEM values. Graphs were generated using GraphPad Prism software Ver. 8.0 (San Diego, California). Statistical analysis was conducted using one-way ANOVA followed by Tukey's Honestly Significant Difference (HSD) post-hoc test from three independent experiments. Statistical significance was found at a *P*-value less than 0.05.

RESULTS

Effects of ECa 233 on the inhibition of KON oral cancer cell proliferation

As seen in Fig. 1A-D and Table 1, after KON cells were incubated with ECa 233 for 24, 48, 72, and 96 h, the percentages of cell viability of KON cells decreased in a concentration- and time-dependent manner. The high concentration of ECa 233 at 50 and 100 µg/mL significantly reduced the percentage of cell viability in 48, 72, and 96 h. Remarkably, the standardized extract of ECa 233 possesses specific cytotoxicity towards oral cancer cells. Based on the results, ECa 233 further demonstrated the characterization and pattern of cell death in the KON cells. Corresponding with the MTT colorimetric results, the optimal concentrations of ECa 233 obtained for further use based on the IC_{50} value concentration of the KON cells in the study are 25, 50, 100, and 200 µg/mL.

Effects of ECa 233 on morphological changes and apoptotic cell death in KON oral cancer cells

As seen in Fig. 2A, the effects of ECa 233 on the morphological alteration and pattern of cell death were identified by bright-field microscope and DAPI and FDA double staining. To characterize the programmed cell death in the ECa 233-induced nuclear condensation, disorganized intracellular compositions, loss of adhesion and integrity, and formation of apoptotic bodies at 25, 50, 100, and 200 µg/mL were associated with apoptosis. Treatment with ECa 233 at 25 and 50 µg/mL for 24 h did not markedly produce observed KON cell death. However, the high concentrations of ECa 233 at 100 and 200 µg/mL triggered cell death (Fig. 2B)

Table 1. Inhibitory concentrations (IC) values of ECa 233 at 25, 50, and 75% on KON cells after treatment for 24, 48, 72, and 96 h. The data are expressed as mean ± SEM, (n = 3).

Time (h)	IC_{25} (µg/mL)	IC_{50} (µg/mL)	IC_{75} (µg/mL)
24	< 1.000	45.08 ± 18.85	82.11 ± 20.85
48	< 1.000	23.73 ± 7.647	51.67 ± 5.897
72	< 1.000	18.82 ± 9.427	48.19 ± 7.142
96	< 1.000	14.72 ± 7.784	38.13 ± 14.99

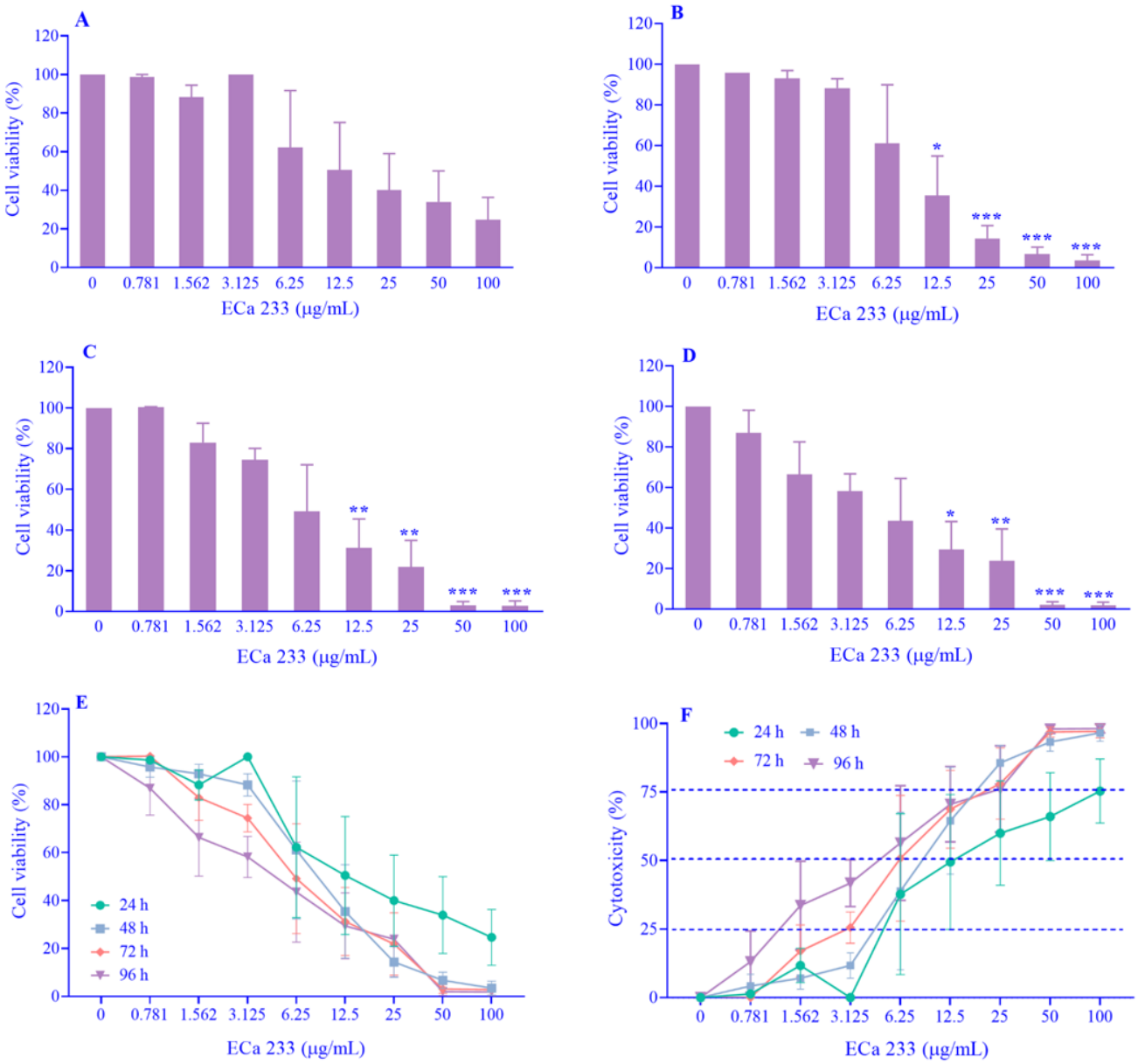

Fig. 1. Effects of ECa 233 on cell viability of KON cells. Cells were treated with ECa at 233 0.78125 - 100 µg/mL for (A) 24, (B) 48, (C) 72, and (D) 96 h. The percentage of cell viability was determined by the MTT colorimetric assay. Graphs were plotted to present the (E) % of the cell viability and (F) % of inhibition. Data are expressed as mean ± SEM from three independent experiments. **P* < 0.05, ***P* < 0.01, and ****P* < 0.001 represent significant differences compared with the control group. ECa 233, Extract of *Centella asiatica*.

Determination of cell death and cells undergoing apoptosis after treating KON cells with ECa 233

As shown in Fig. 3, to confirm the anticancer activity of the ECa 233-induced apoptosis phenomenon in the KON cells, Hoechst 33258 and AO were selected as double-staining fluorescent dyes to explore the apoptotic events. The stained cells were observed using an inverted fluorescent microscope. The KON cells treated with 25 and 50 µg/mL increased in terms of the number of cell deaths as compared to the respective control cells. The nuclei of untreated cells were found to be normal in both size and cell structure and shape, while the KON cells treated with 100 and 200 µg/mL presented the dead cells, apoptotic cells, and alteration of the normal cell structure of KON cells, such as fragmentation of nuclei and nucleus condensation. These results suggest that ECa 233 has the potential to trigger KON cell death and apoptosis.

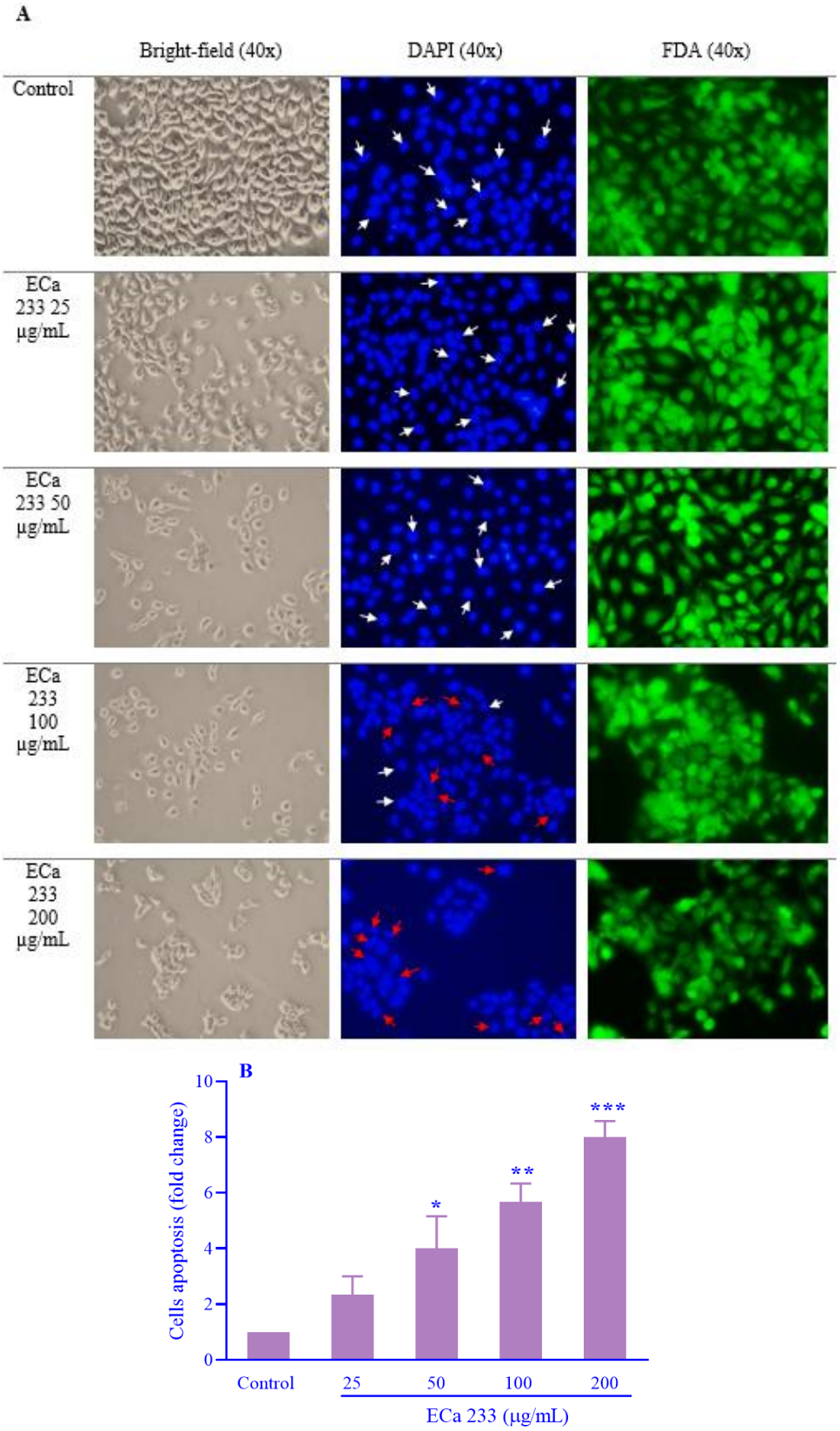

Fig. 2. (A and B) The effects of ECa 233 on the morphological changes and apoptotic cell death of KON cells. Cells were treated with 25, 50, 100, and 200 µg/mL of ECa 233 for 24 h. The KON cells were observed for the pattern of cell death by an inverted microscope (40×). Cytomorphological changes were investigated using an inverted fluorescent microscope (40×). The data are expressed as mean ± SEM, n = 3. **P* < 0.05, ***P* < 0.01, and ****P* < 0.001 represent significant differences compared with the control group. White arrows and red arrows denote normal and apoptotic nuclei, respectively. ECa 233, Extract of *Centella asiatica.*

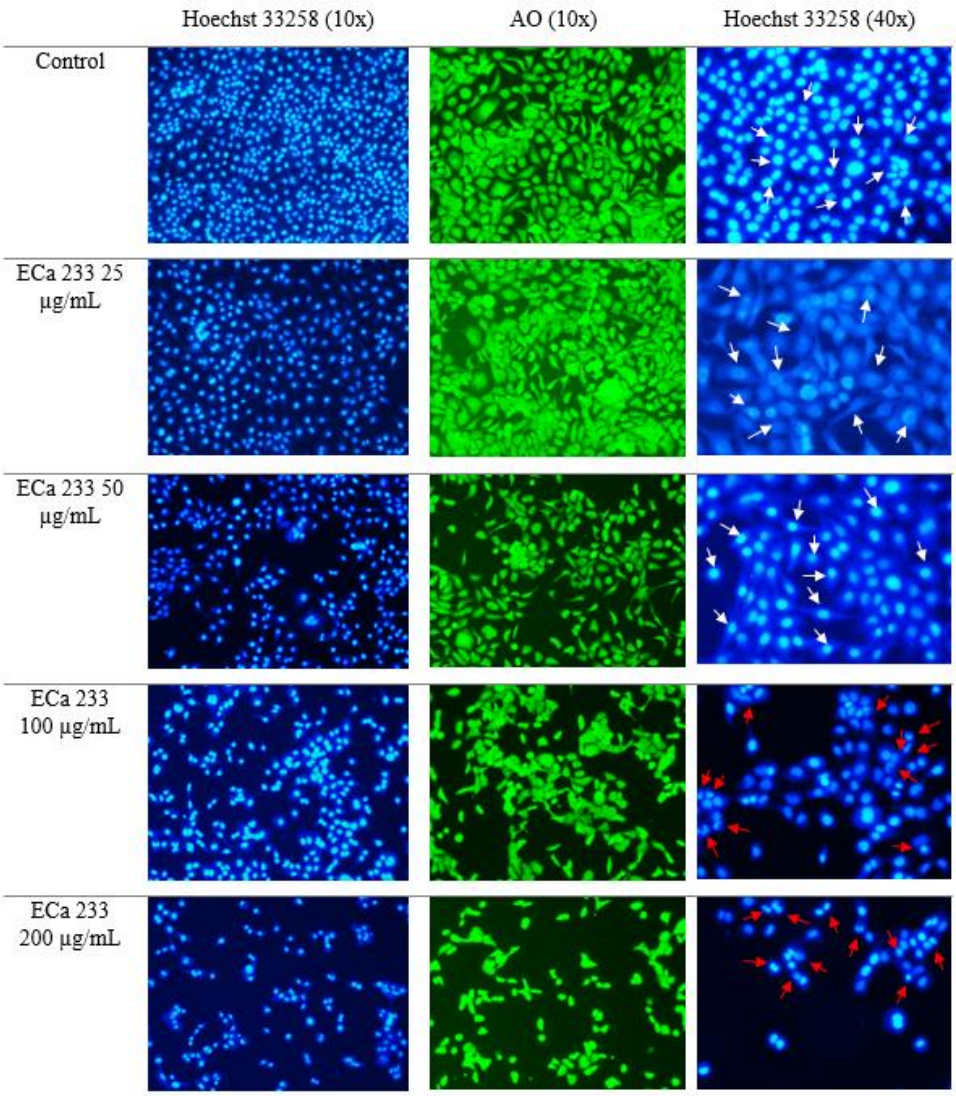

Fig. 3. The effects of ECa 233 in triggering apoptotic events in KON cells. The cells were treated with ECa 233 at 25, 50, 100, and 200 µg/mL for 24 h. The KON cells were characterized as apoptotic cells using an inverted microscope (40×). Cells were fixed with 4% paraformaldehyde for 15 min and permeabilized with 0.2% Triton®-X-100, then stained with Hoechst 33258 and 5 µL of AO for 30 min in a dark room. Apoptosis of the KON cells was investigated using an inverted fluorescent microscope (40x). White arrows and red arrows denote normal and apoptotic nuclei, respectively. AO, Acridine orange; ECa 233, extract of *Centella asiatica*.

Induction of cell apoptosis after treatment with ECa 233 in KON oral cancer cells by annexin V-FITC staining

To detect KON cells during the initiation of apoptosis after induction with 25, 50, 100, and 200 µg/mL of ECa 233, as illustrated in Fig. 4A and B, in non-fixed cells, the KON cells were detected as having the number of cell apoptosis that was greater in 100, 50, and 25 µg/mL, respectively, compared with the control. In the fixed cells, annexin V-FITC could penetrate whole cells, presenting at 200 µg/mL of ECa 233, actual induction of the loss of cell membrane, cell integrity, and disruption of the normal cell structure. These findings indicate that ECa 233 induced the KON oral cancer cells to undergo apoptosis.

Effects of ECa 233 on ROS generation in KON cells

To elucidate whether ROS generation is responsible for ECa 233-induced cell death and may function as a mechanism that mediates cells undergoing apoptosis, as shown in Fig. 5A and B, the results demonstrated that ECa 233 potently increased the ROS production in KON cells compared to the control group. Therefore, the ROS generation inside the KON cells treated with ECa 233 may be one possible underlying mechanism to explain the related cell death.

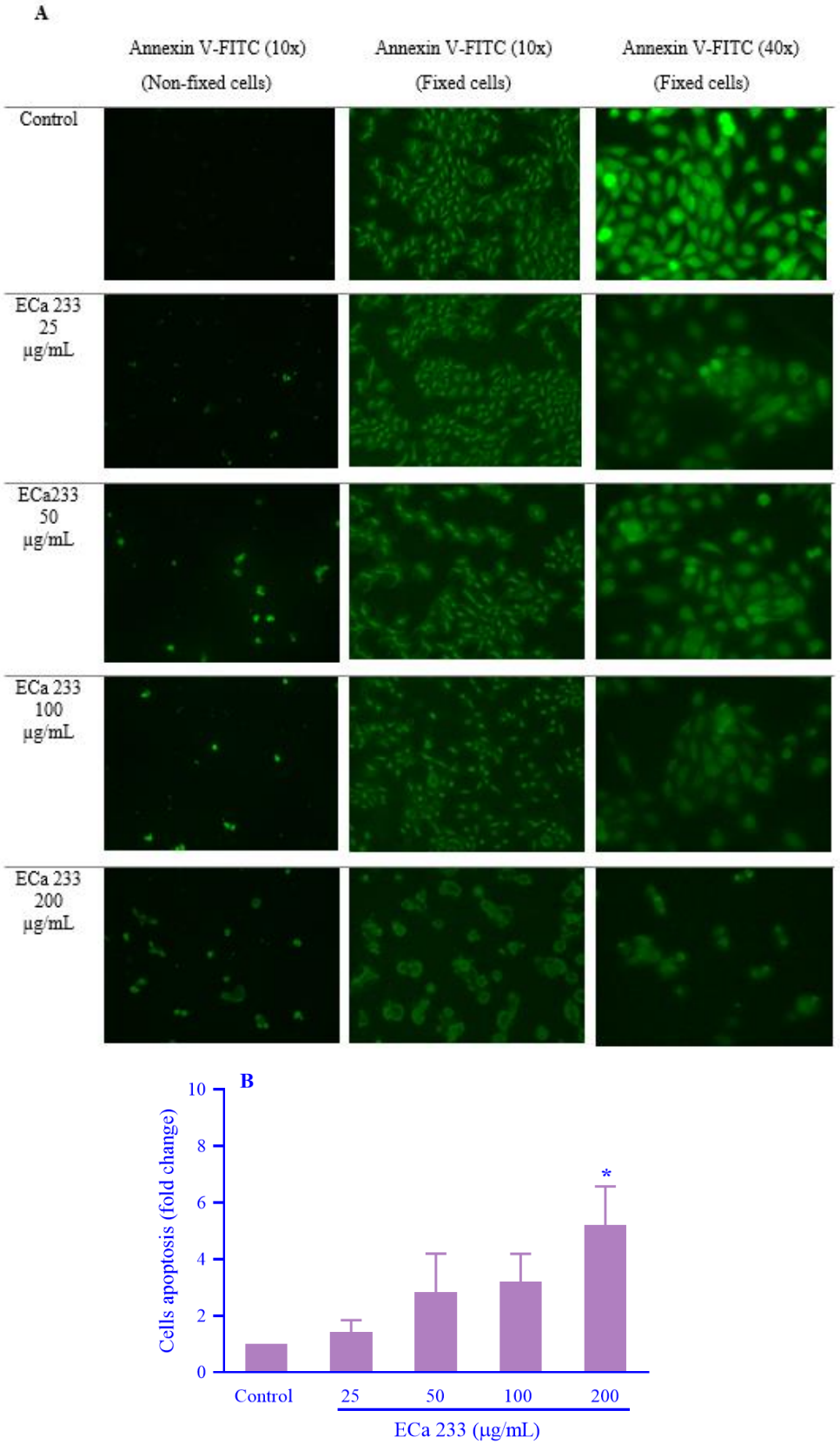

Fig. 4. (A and B) The effects of ECa 233 on the induction of apoptosis of KON cells after treatment with ECa 233. Cells were treated with ECa 233 at 25, 50, 100, and 200 µg/mL for 20 h. KON cells were observed for the pattern of cell death by a bright field microscope (40×) and annexin V-FITC fluorescent color staining. Fixed cells and non-fixed cells on sterile coverslips were stained with annexin V-FITC and cell apoptosis was determined by a fluorescent microscope at 10× and 40× objective magnification. The results were presented as relative to cell apoptosis, n = 3. The data are expressed as mean ± SEM, n = 3. *$P < 0.05$ represents the significant difference in comparison with the control group. ECa 233, Extract of *Centella asiatica.*

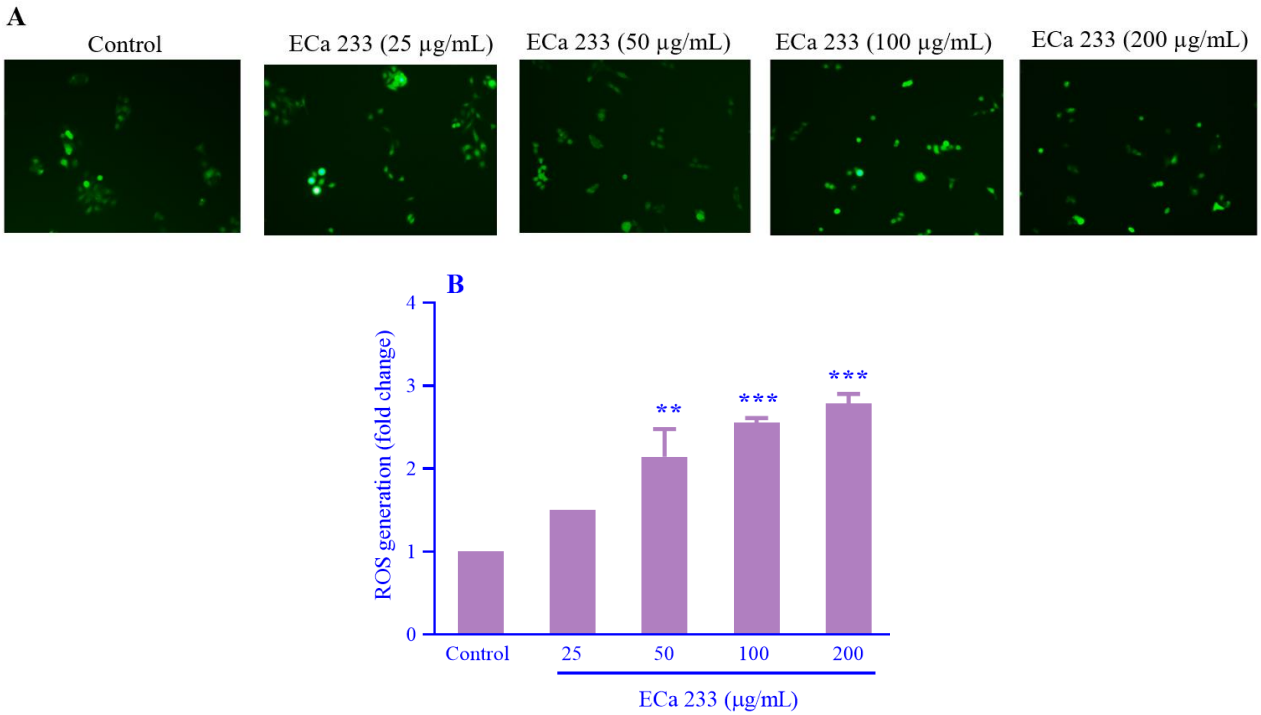

Fig. 5. Determination of the ROS generation in ECa 233-treated KON cells The data are expressed as relative to ROS generation and presented as mean ± SEM, n = 3. $^{**}P < 0.01$ and $^{***}P < 0.001$ represent the significant differences in comparison with the control group. ECa 233, Extract of *Centella asiatica;* ROS, reactive oxygen species.

Determination of cell death in KON cells by flow cytometry analysis

PI staining and flow cytometry were utilized to determine the cell death in the KON cells treated with ECa 233. PI staining was used to investigate the aberrant alteration of the nucleus by binding the DNA inside the KON cells. As depicted in Fig. 6A and B, the results demonstrated that ECa 233-induced cell death occurred in a concentration-dependent manner after being treated with 25, 50, 100, and 200 µg/mL of ECa 233 for 24 h.

Cell cycle analysis by flow cytometry

Cell cycle arrest is one of the important mechanisms of anticancer agents that facilitates their inhibitory proliferation rate. Therefore, the effect of ECa 233 on the cell cycle progression of KON cells was examined in the present study. As shown in Fig. 7A and B, the results demonstrate that the number of KON cells increased in the sub-G phase of the cell cycle at 25 µg/mL of ECa 233, possibly inducing sub-G arrest, which prevents KON cells from entering the subsequent phases of the cell cycle. The proportions of KON cells in the sub-G phase significantly increased at the concentrations of 50 and 100 µg/mL. However, the high concentration of ECa 233 at 200 µg/mL induced cell death and decreased the progression of KON cells to cell cycle division.

Inhibitory effect of ECa 233 on the migratory capacity of KON oral cancer cells

Assessment of the migratory ability of KON cells after treatment with ECa 233 at 25, 50, 100, and 200 µg/mL was done by the wound scratch assay, monitored at time 0, 18, 24, and 48 h. The % of open wound areas at time 0 h after generating the wound were 77.62 ± 0.8225, 80.32 ± 1.443, 75.91 ± 1.675, 73.55 ± 0.171, and 73.48 ± 1.392, respectively. As shown in Fig. 8A and B, in the control group, the cells sustained migratory capacity in migration to the center of the straight line of the open wound after 24 and 48 h treatment, in contrast, the KON cells treated with ECa 233 at 25, 50, 100, and 200 µg/mL showed significantly reduced cell migration after treatment for 18, 24, and 48 h. The % of open wound areas at time 18 h were 67.1 ± 0.477, 70.21 ± 0.4853, 71.68 ± 0.5467, 71.65 ± 0.1597, and 71.79 ± 0.7606, respectively. The % of open wound areas at time 24 h were 66.03 ± 0.9951, 72.13 ± 0.607, 71.78 ± 0.8222, 70.2 ± 0.1604, and 70.89 ± 1.777, respectively. The % of open wound areas at time 48 h were 66.81 ± 2.552, 69.47 ± 1.497, 71.22 ± 1.105, 73.05 ± 0.3555, and 71.59 ± 0.4402, respectively. These results demonstrated that ECa 233 could modulate the migration ability of KON cells.

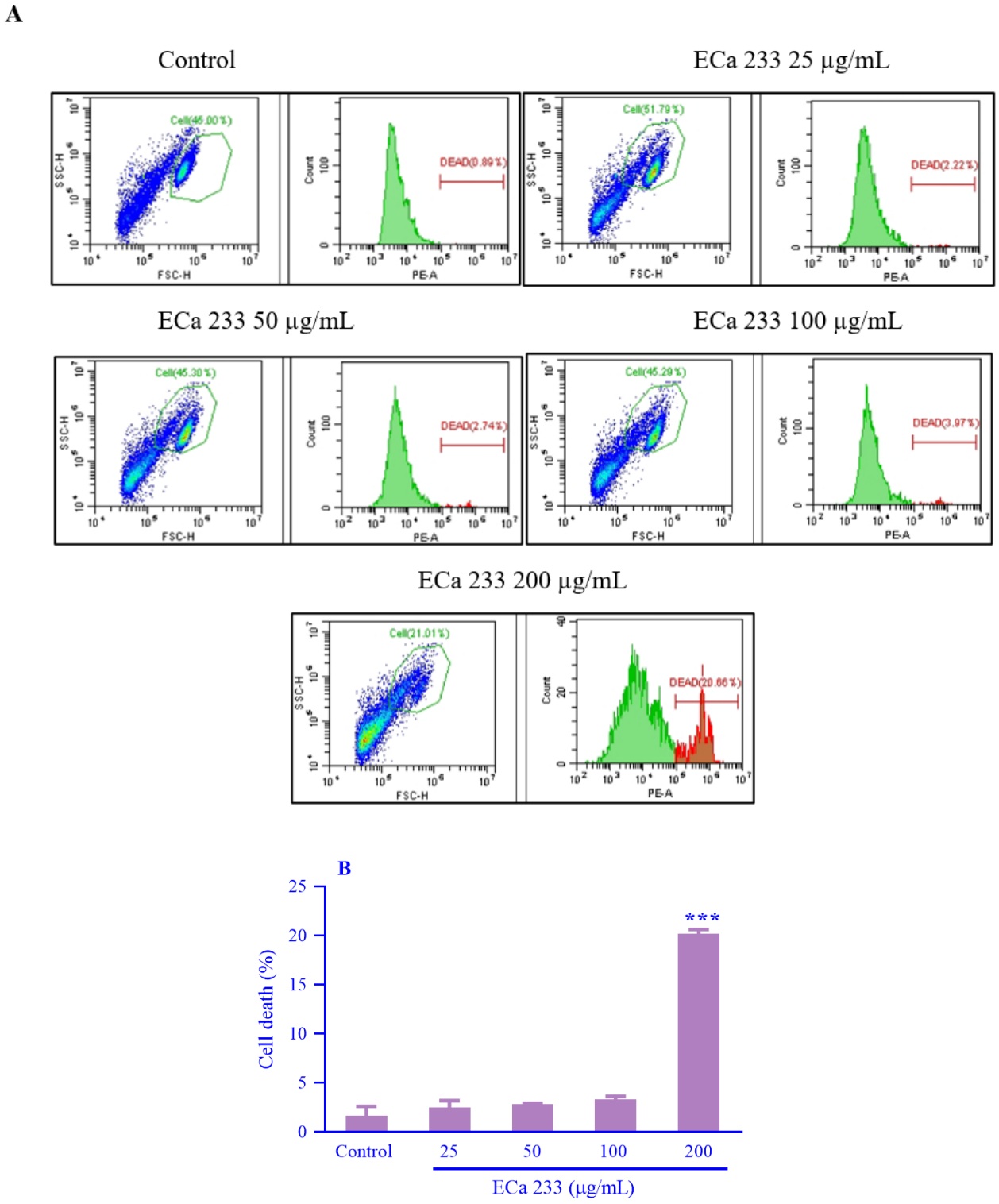

Fig. 6. (A and B) Estimation of KON cell death after treatment with ECa 233 at 25, 50, 100, and 200 µg/mL using propidium iodide staining and flow cytometry. Data are presented as mean ± SEM, n = 3. ***$P < 0.001$ represents the significant difference in comparison with the control group. ECa 233, Extract of *Centella asiatica.*

Anti-habitual effects of ECa 233 on colony-forming and metastatic behavior of KON oral cancer cells

To further evaluate the anticancer potential of ECa 233 on KON cells, a colony formation assay was carried out. Typically, cancer cells have a propensity to grow and spread in colonies in contact with neighboring cells, thereby losing the interconnection with the adjacent cells, which results in the departure of the cancer cells. As demonstrated in Fig. 9A and B, the results reveal that the

percentages of colony formation in ECa 233-treated cells remarkably decreased in comparison with the control group. Critical events in cancer progression comprise migration and invasion, especially the invasion, which is the principal step in the metastasis cascade, when cancer cells require the ability to move, degradation of surrounding tissue, and extracellular matrix penetration into the circulatory and lymphatic systems, thereby reaching other parts of the body. In this regard, the metastatic drivers of cancer cells are constitutively interesting targets for cancer therapy. Transwell migration and Matrigel invasion assays were carried out, and the percentages of cells decreased significantly in all treated groups compared with the control group (Fig. 9A and C). The percentages of cell invasion were also reduced after treatment with the different concentrations of ECa 233 compared with the control group (Fig. 9A and D).

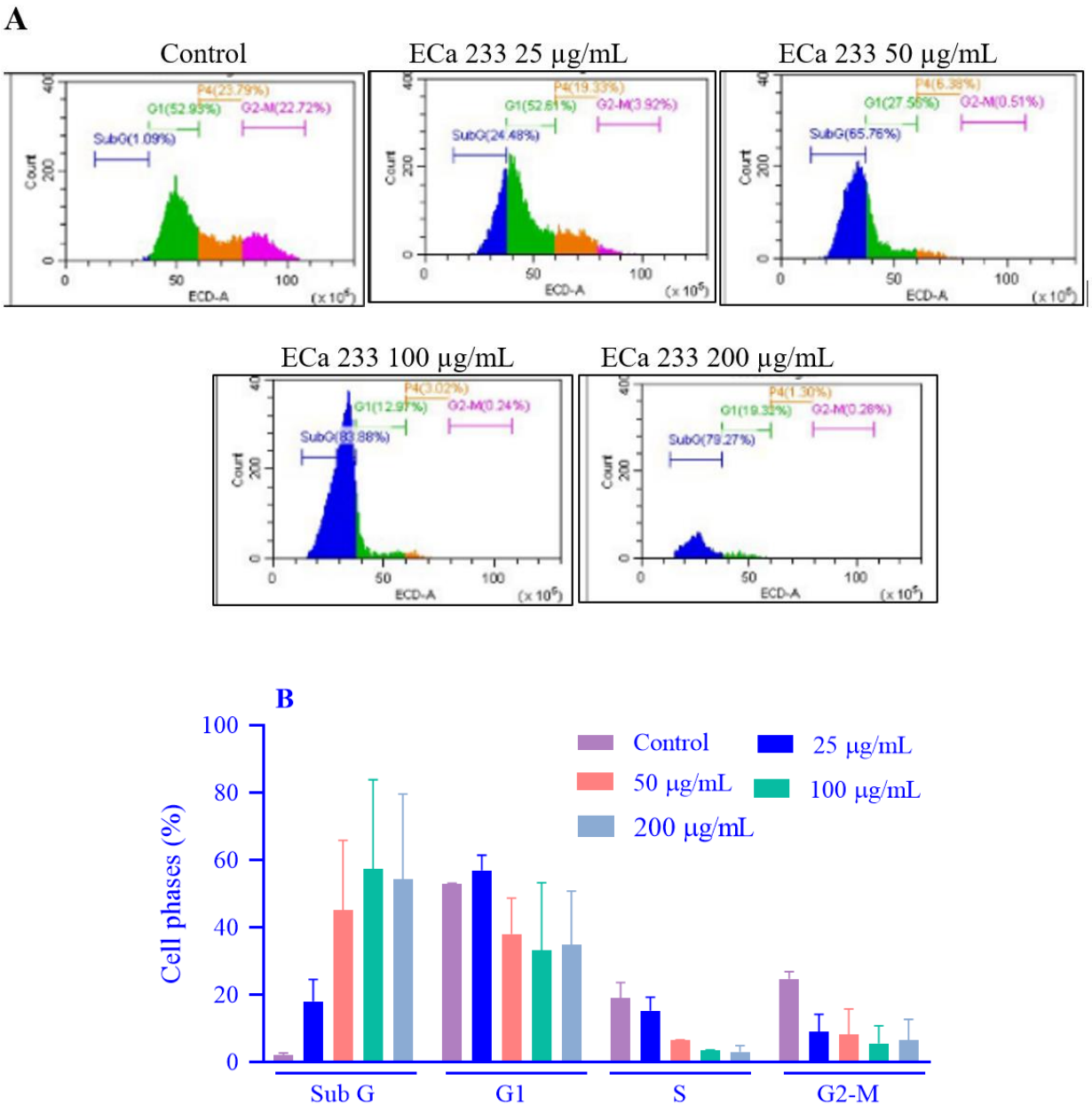

Fig. 7. (A and B) Flow cytometry analysis of cell cycle arrest in KON cells treated with ECa 233 for 24 h. The data from the representative flow cytometry histogram, for the cell cycle phase (% in Sub G, G1, S, and G2-M phases) were presented as mean ± SEM, n = 3. ECa 233, Extract of *Centella asiatica.*

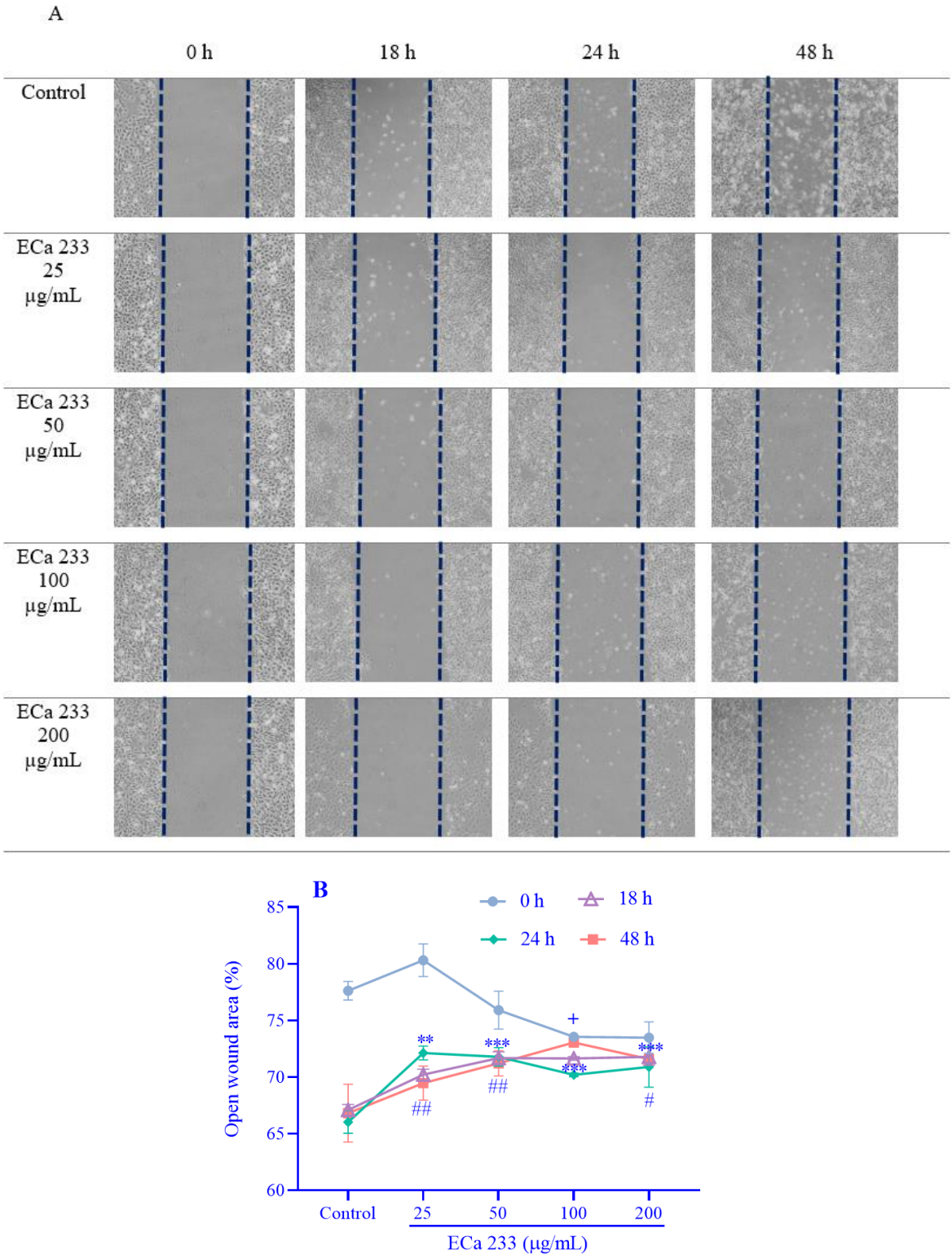

Fig. 8. The 100% confluent monolayer of KON cells was used to generate a straight line by scratching with a 200 µL pipette tip. The KON cells were incubated with DMEM supplemented with 5% FBS containing ECa 233 at 25, 50, 100, and 200 µg/mL for 18, 24, and 48 h. Cells were captured with a bright field microscope at 4× objective magnification. The results were expressed as % of wound closure (n = 3). $^{**}P < 0.01$ and $^{***}P < 0.001$ indicate significant differences from the control at time 18 h; $^{\#}P < 0.05$ and $^{\#\#}P < 0.01$ versus the control at time 24 h, and $^{+}P < 0.05$, significantly different from the control at time 48 h. ECa 233, Extract of *Centella asiatica*; DMEM, Dulbecco's modified eagle's medium; FBS, fetal bovine serum.

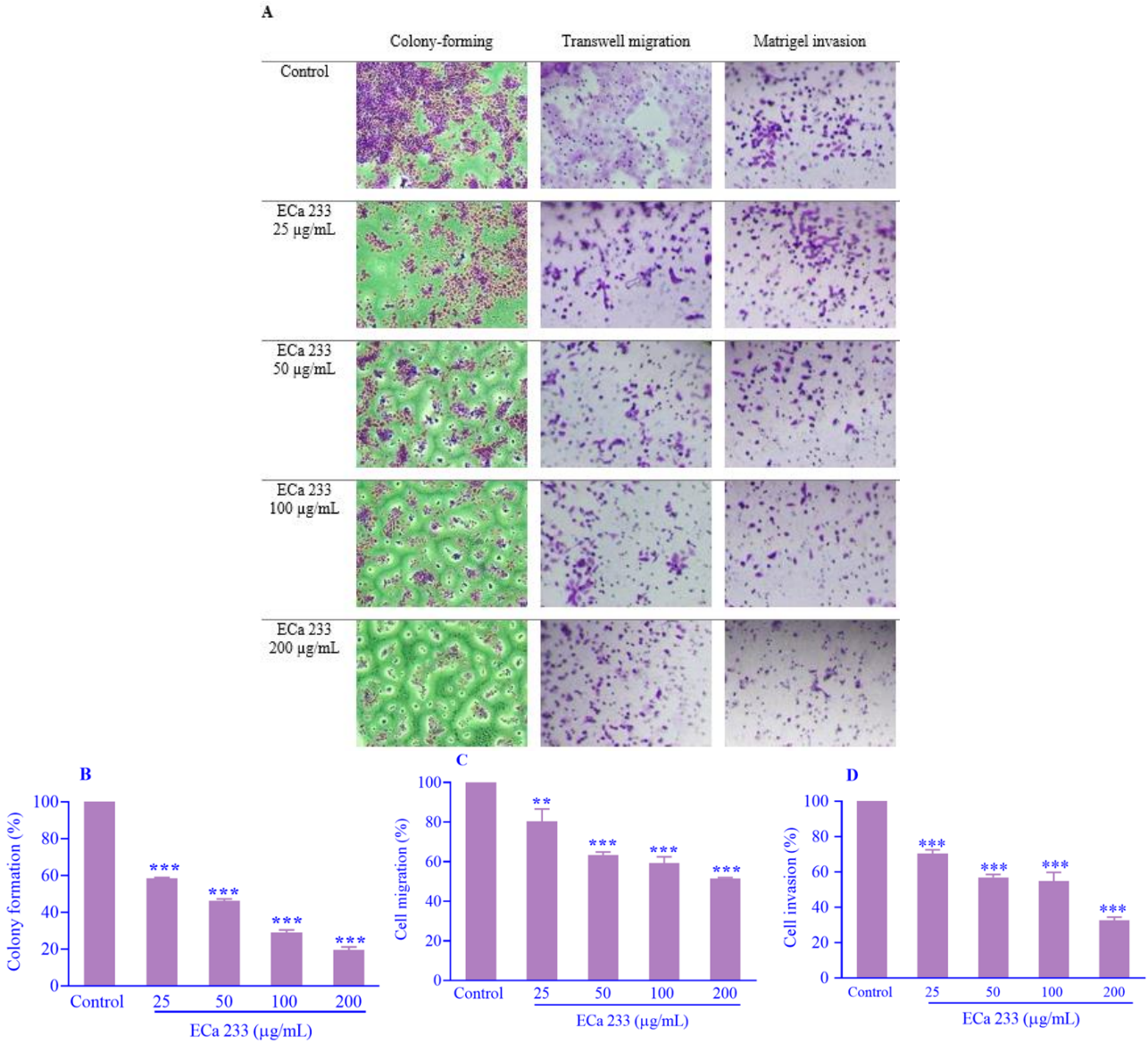

Fig. 9. (A-D) Effects of ECa 233 on colony formation, cell migration, and cell invasion in KON cells. The KON cells were treated with ECa 233 (25, 50, 100, and 200 µg/mL) for 24 h and then washed with 1× PBS and further cultured in a 12-well plate for 7 days. For the migrative and invasive experiments, the KON cells were re-suspended within the serum-free medium before being seeded in the upper chamber of the system with the fixed concentrations of ECa 233 (25, 50, 100, and 200 µg/mL) for 48 h. The lower system was filled with DMEM media supplemented with 10% FBS acting as a chemo-attractant. Migrated and invaded cells were fixed with ice-cold methanol and stained with crystal violet. The KON cells were photographed using an inverted microscope at 10× magnification. The results were presented as a percentage of colony formation, cell migration, and cell invasion. Data are expressed as mean ± SEM, n = 3. $^{**}P < 0.01$ and $^{***}P < 0.001$ indicate the significant differences in comparison with the control group. ECa 233, Extract of *Centella asiatica*; DMEM, Dulbecco's modified eagle's medium; FBS, fetal bovine serum.

Effects of ECa 233 on cell migration and invasion of KON oral cancer cells in E_2-induced condition

To investigate the anticancer potential of ECa 233 on cell migration and invasion of KON cells in an E_2-induced condition, E_2 was used as a chemo-attractant agent as well as for mimicking an E_2 surge in the body. In the control group, E_2 was able to induce cell migration and invasion from the upper surface to the lower chamber of the system. As shown in Fig. 10A and B, in the presence of ECa 233 at 25, 50, 100, and 200 µg/mL, the percentages of cell migration in the E_2-induced condition quite decreased compared to the control group. Moreover, ECa 233 treatment significantly reduced the percentages of cell invasion in the E_2-induced condition in comparison with the control group (Fig. 10A and C). These results demonstrated that ECa 233 can modulate migration and invasion capacity in E_2-induced conditions.

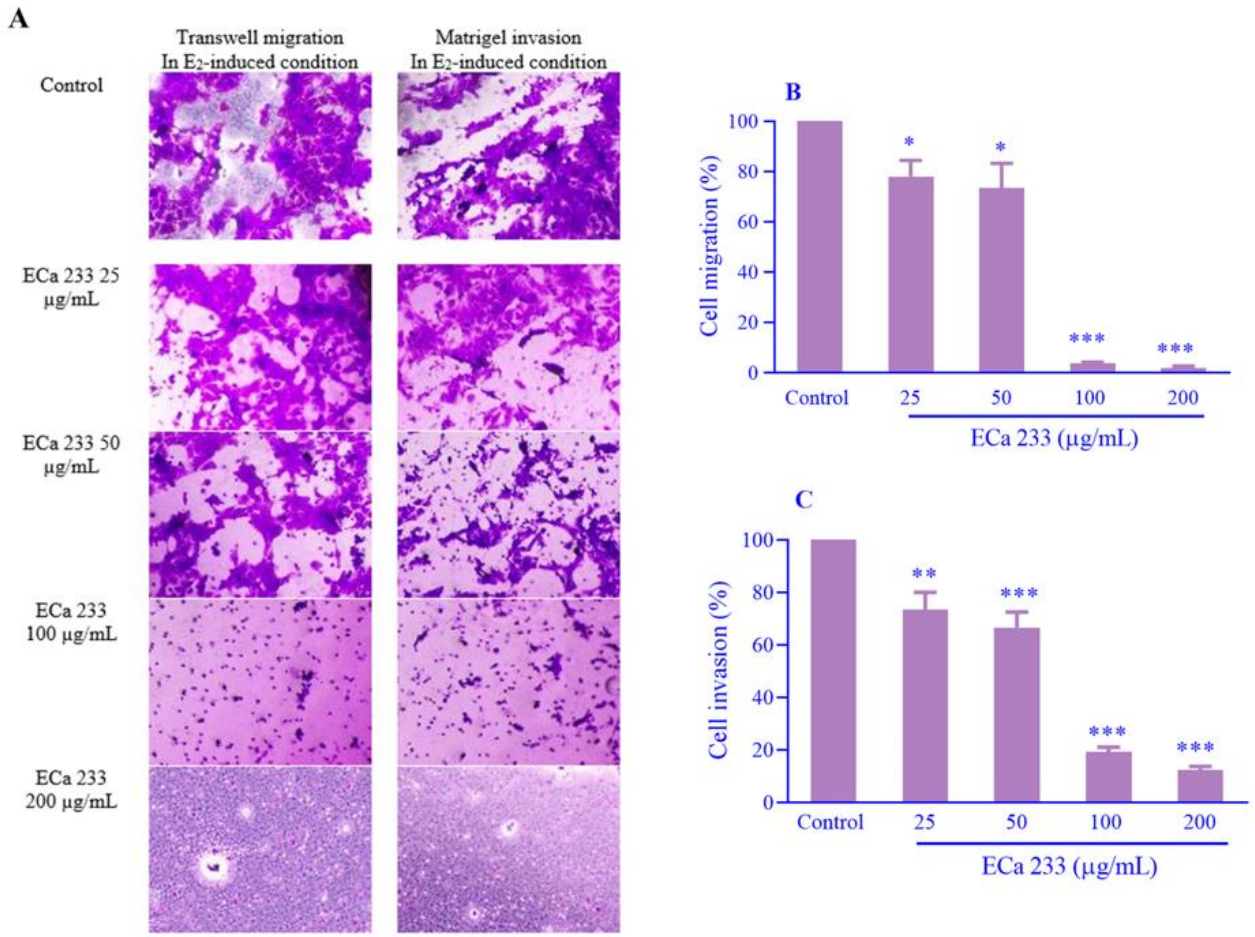

Fig. 10. (A-C) Effects of ECa 233 on cell migration and cell invasion of KON cells in E_2-induced condition. For the migrative and invasive experiments in the E_2-induced condition, the KON cells were re-suspended with phenol red-free DMEM medium before being added into the upper chamber of the system in the fixed concentrations of ECa 233 (25, 50, 100, and 200 µg/mL) for 48 h. The lower system was filled with 500 µL phenol red-free DMEM media + 5 µg/mL of E_2 acting as a chemo-attractant. Migrated and invaded cells were fixed with ice-cold methanol and stained with crystal violet. The KON cells were captured using an inverted microscope at 10× magnification. The results were presented as a percentage of cell migration and cell invasion in the E_2-induced condition. Data are expressed as mean ± SEM, n = 3. *P < 0.05, **P < 0.01, and ***P < 0.001 indicate the significant differences in comparison with the control group. ECa 233, Extract of *Centella asiatica*; DMEM, Dulbecco's modified eagle's medium; FBS, fetal bovine serum; E_2, beta-estradiol.

Determination of TEER values and multicellular cancer spheroids formation after induction of KON cells with ECa 233

The effects of ECa 233 on the TEER values of the KON cells were also investigated after induction with ECa 233 for 24 h. As seen in Fig. 11A and B, treatment with ECa 233 significantly increased the TEER values compared with the control group. These results indicated that ECa 233 may change the cell permeability and alter the integrity of cellular barriers, resulting in ECa 233 moving inside the KON cells. The *in vitro* multicellular cancer spheroids have long been considered a good model in experiments for determining the anticancer activity and reflecting the *in vivo* tumor behavior and growth. The KON oral cancer spheroids were tested to determine the responses to 25, 50, 100, and 200 µg/mL of ECa 233 for 24 h. Treatment with different concentrations of ECa remarkably minimized the % KON oral cancer spheroids cell viability after examination using the PrestoBlue™ method Fig. 11A and C. These results suggest that ECa 233 can modulate aggressive cancer behavior in KON cells by minimizing the proliferative capacity.

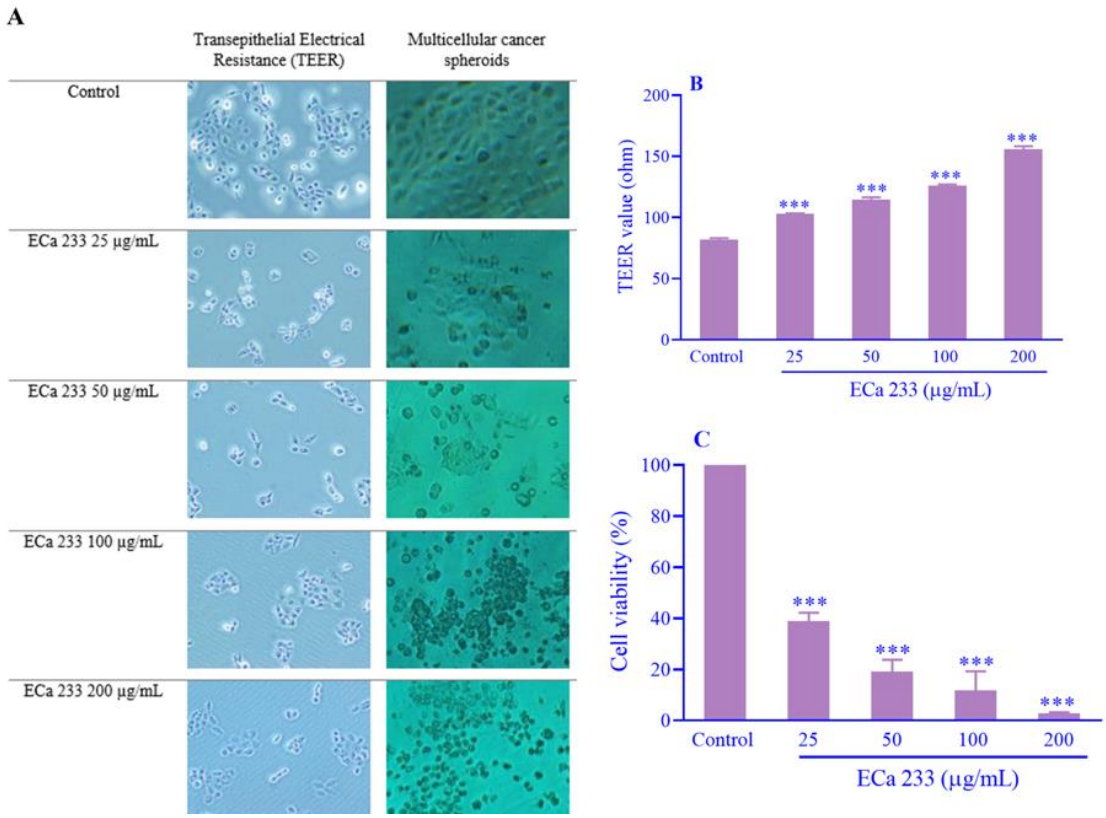

Fig. 11. (A) Effects of ECa 233 on TEER values in KON cells. (B) To quantify the TEER value as an indicator of the integrity of the cell barrier and evaluate the transport of ECa 233 to KON cells, the KON cells were seeded in a 6-well plate for 24 h in a 5% CO_2 incubator. After induction of the KON cells with ECa 233 for 24 h, the cell monolayers were measured for TEER values with a Millicell® ERS-2 voltohmmeter. The KON cells were cultured in a 96-well round bottom plate to allow replication to multi-cellular spheroids for 4 days. (C) The KON oral multi-cellular spheroids were tested for the response to 25, 50, 100 and 200 µg/mL of ECa 233 for 24 h. The PrestoBlue assay was used to determine the % cell viability. The plates were read for fluorescence intensity of resorufin with a fluorescence microplate reader at 570 nm. Data are expressed as mean ± SEM, n = 3. ***$P < 0.001$ Indicates significant differences in comparison with the control group. ECa 233, Extract of *Centella asiatica*; TEER, transepithelial electrical resistance.

The safety profile of ECa 233 on the cell viability of MRC-5 normal fibroblast cells

To investigate the harmful effects of ECa 233 on the cell viability of MRC-5 normal fibroblast cells after treatment with ECa 233 at 0.78125, 1.5625, 3.125, 6.25, 12.5, 25, 50, and 100 µg/mL for 8, 22, and 30 h, the viability of normal cells was monitored using the MTT colorimetric assay. As seen in Fig. 12A and B, after incubation with ECa 233 for 8 h, the percentage of cell viability in MRC-5 cells was approximately 90-100%, and there were minimal effects on the cell growth. However, after incubation with ECa 233 for 22 and 30 h (Fig. 12A, C, and D), the percentages of cell viability of the MRC-5 cells decreased after exposure to the high concentration of ECa 233. Notably, there were no observed morphological changes in the MRC-5 normal fibroblast. These results suggest that the specific toxicity of ECa 233 to KON oral cancer cells, however non-toxic to normal cells. These data indicate the safety profile of ECa 233 for normal cells and thus, it has the potential to be beneficial for use in drug development.

Pharmacokinetics profiles of madecassoside and asiaticoside prediction

The pharmacokinetic properties of the plant extracts were investigated to predict the toxicity and significant pharmacological effects after administration. The pharmacokinetic profiles (absorption, distribution, metabolism, excretion, and toxicity; ADMET) of madecassoside were carried out using *in silico* analysis (pkCSM program) as shown in Table 2. The *in-silico* estimation of ADMET properties demonstrated that human intestinal absorption of madecassoside is 23.756%.

A

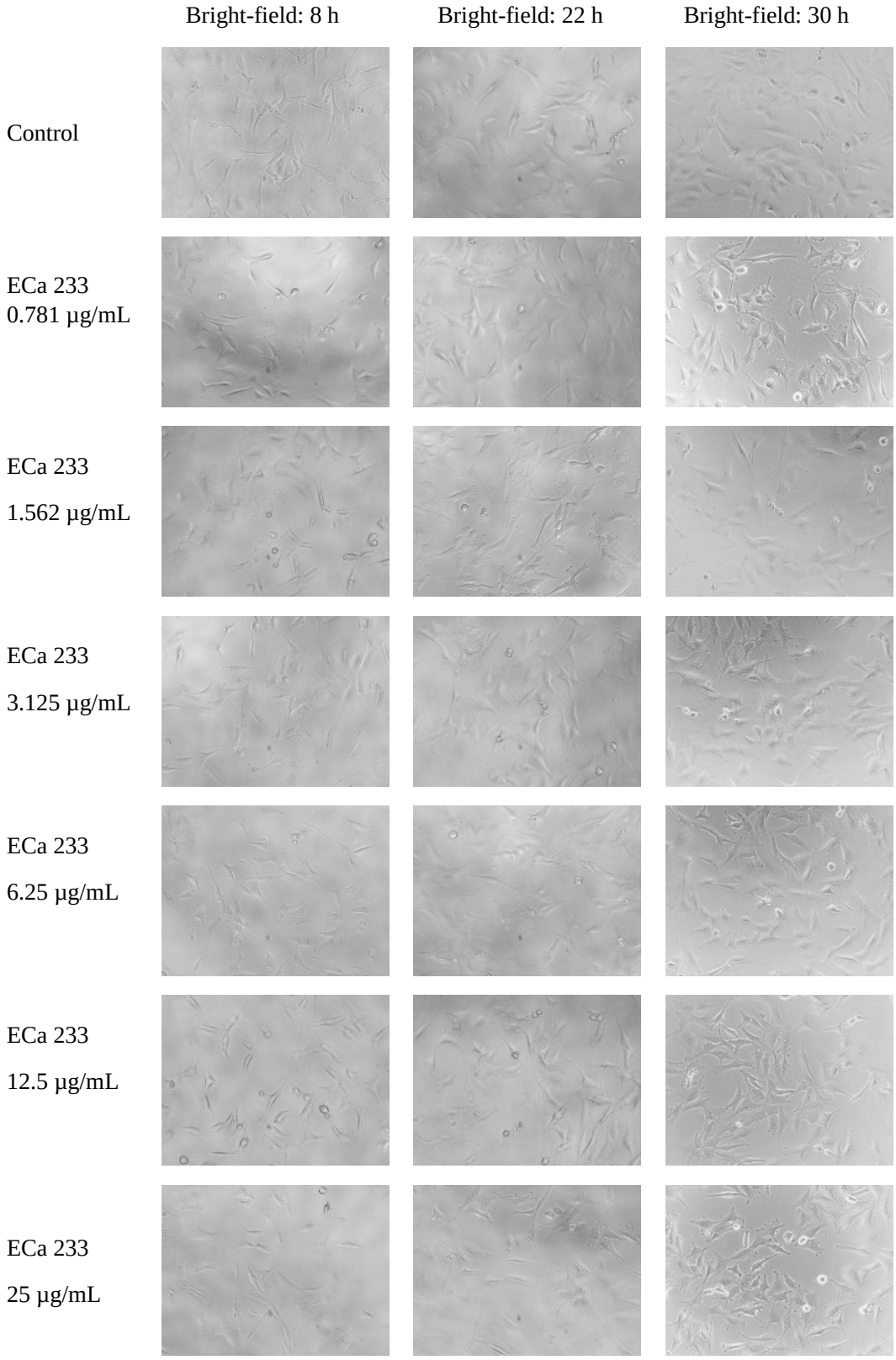
Bright-field: 8 h
Bright-field: 22 h
Bright-field: 30 h
Control
ECa 233
0.781 µg/mL
ECa 233
1.562 µg/mL
ECa 233
3.125 µg/mL
ECa 233
6.25 µg/mL
ECa 233
12.5 µg/mL
ECa 233
25 µg/mL

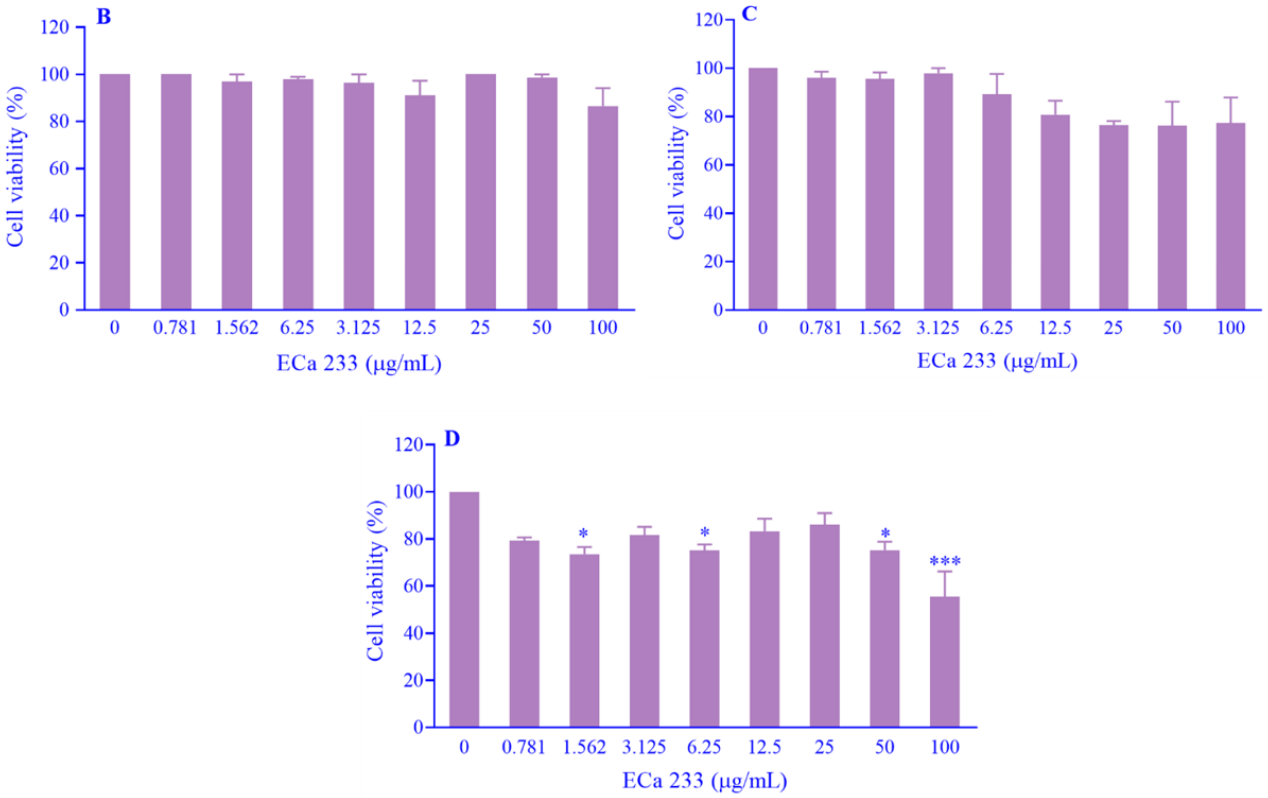

Fig. 12. Effect of ECa 233 on cell viability of MRC-5 normal fibroblast cells. (A) MRC-5 cells were treated with ECa 233 at 0.78125, 1.5625, 3.125, 6.25, 12.5, 25, 50, and 100 µg/mL for (B) 8 h, (C) 22 h, and (D) 30 h. The percentages of cell viability were determined by the MTT colorimetric assay. Data are expressed as mean ± SEM, n = 3. **P* < 0.05 and ****P* < 0.001 indicate significant differences in comparison with the control group. ECa 233, Extract of *Centella asiatica*.

Table 2. Pharmacokinetic profile of madecassoside predicted using *in silico* analysis (pkCSM program).

Pharmacokinetic properties	Model name	Predicted value
Absorption	Intestinal absorption (human)	23.756 (% absorbed)
Distribution	VDss (human)	-0.546 (log L/kg)
	BBB permeability	-1.975 (log BB)
Metabolism	CYP2D6 substrate	No
	CYP3A4 substrate	No
	CYP1A2 inhibitor	No
	CYP2C19 inhibitor	No
	CYP2C9 inhibitor	No
	CYP2D6 inhibitor	No
	CYP3A4 inhibitor	No
Excretion	Total clearance	0.233 (log mL/min/kg)
	Renal OCT2 substrate	No

VDss, Volume of distribution at steady state; BBB, blood-brain barrier; CYP, cytochrome P-450; OCT2, organic cationic transporter 2.

The steady-state volume of distribution of madecassoside was -0.546 (log L/kg). The blood-brain barrier permeability was -1.975 (log BB). Madecassoside revealed no effect on most CYP enzymes in hepatocytes, which suggests that it will not affect the metabolism of other drugs. The excretion (total clearance) of madecassoside was 0.233 (log mL/min/kg).

The pharmacokinetic profiles (ADME) of asiaticoside were determined using *in silico* analysis (pkCSM program), as shown in Table 3. The *in-silico* evaluation of ADMET properties demonstrated that human intestinal absorption of asiaticoside is 29.201%. The steady-state volume of distribution of asiaticoside was -0.578 (log L/kg). The blood brain barrier permeability was -1.884 (log BB).

Table 3. Pharmacokinetic profile of asiaticoside predicted using *in silico* analysis (pkCSM program)

Pharmacokinetic properties	Model name	Predicted value
Absorption	Intestinal absorption (human)	29.201 (% Absorbed)
Distribution	VDss (human)	-0.578 (log L/kg)
	BBB permeability	-1.884 (log BB)
Metabolism	CYP2D6 substrate	No
	CYP3A4 substrate	No
	CYP1A2 inhibitor	No
	CYP2C19 inhibitor	No
	CYP2C9 inhibitor	No
	CYP2D6 inhibitor	No
	CYP3A4 inhibitor	No
Excretion	Total clearance	0.227 (log mL/min/kg)
	Renal OCT2 substrate	No

VDss, Volume of distribution at steady state; BBB, blood-brain barrier; CYP, cytochrome P-450; OCT2, organic cationic transporter 2.

Asiaticoside revealed no effect on most of the CYP enzymes in the hepatocytes. The excretion (total clearance) of asiaticoside was 0.227 (log mL/min/kg). OCT2 is predominantly a transporter located in the proximal tubule epithelial cells and plays a role in the disposition and clearance of cationic substrates that are positively charged at the physiological pH level, which may affect the uptake of several pharmaceutical products. Madecassoside and asiaticoside are not to be used as an OCT2 substrate, as they do not exhibit drug-drug interactions that reduce the renal clearance of OCT2 substrates.

DISCUSSION

Oral cancer is the most common general type of cancer that occurs as a significant clinical burden worldwide. Delayed diagnosis is a problem affecting the 5-year survival rates of patients; however, the survival rate is 80-90% if the disease is detected early (30,31). Strikingly, about 50% of OSCCs are ongoingly being identified at an advanced cancer stage, with enlarged tumor size (i.e. T3/T4), and 47% also harbor an N+ status. About one-half of oral cancers are diagnosed at the advanced stage (32,33). The search for a promising new active compound that can be found in traditional plants has thus been of interest. Natural compounds seem to be an appropriate option for the prevention and treatment of cancer, due to their exhibited cytotoxic and chemoprevention effect on tumor cells, which mainly act through induction of apoptosis (34,35). *Centella asiatica* is a local plant in Thailand that exhibits a wide range of beneficial biological properties, including wound healing, anti-inflammation, and neuroprotective effects (36,37). ECa 233 is a standardized extract of *Centella asiatica* and is of interest for clinical trial studies because its pharmacokinetic profile has the potential for investment in the clinical research and manufacturing levels (38). However, the potential of ECa 233 toward inhibition of KON cells has not been elucidated. In this study, the anticancer effects of ECa 233 on KON cells, a well-known type of oral cancer cells, were investigated. Our results demonstrated that ECa 233 has selectiveness in inhibiting the growth of KON cells in the microgram doses. The sensitivity of KON cells to ECa 233 is concentration- and time-dependent after being treated with ECa 233 for 24, 48, 72, and 96 h, whereas ECa 233 did not significantly affect the cell viability of MRC-5 cells (Fig. 12). The different sensitivity to ECa 233 between KON cells and MRC-5 cells suggests the specificity of ECa 233 on abnormal cells. This is in agreement with our previous reports that demonstrated the cytotoxicity of ECa 233 in SW-620 colorectal cancer cells (39). These results prove its potential value for anticancer drug development.

Apoptosis is the sequential process of cell death, which provides maintenance of the homeostatic balance and plays a pivotal role in the elimination of non-essential cells by the phagocytosis mechanism. The aberrancy in the apoptosis-controlling mechanism can lead to

the progression of cancer and autoimmune diseases (40,41). Novel alternative medicinal plants and chemical constituents derived from natural products are required to overcome dysfunction and dysregulated apoptosis cascades, increase therapeutic efficacy, and decrease cancer recurrence. The induction of apoptosis in cancer is one way to resolve the uncontrolled proliferative cells. In this study, treatment of KON cells with ECa 233 induced apoptosis with characteristics featuring nuclear blebbing and condensation, as well as loss of cell organization. The morphology of KON cells treated with high concentrations of ECa 233 was aberrantly altered from spindle-like to spherical shapes and was also made to lose their attachment to the culture plate. The rates of apoptotic cells increased in the KON cells treated with the high concentrations of ECa 233, suggesting apoptotic cell death. These results indicate that ECa 233 inhibits the growth of KON cells by inducing cell apoptosis. The possible mechanism involved in cell death and apoptosis was thus elucidated. The results demonstrated that ECa 233 acts as an inducer in generating ROS production in KON cells when compared with the control cells. ROS generation after induction of KON cells with ECa 233 is responsible as a mechanism associated with cell apoptosis and cell death. Cell division is controlled by regulatory proteins in the cell cycle process. Uncontrolled cell division and proliferation is a major feature of cancer. The mechanism of events is associated with the mutation of cell cycle regulatory genes and proteins, which are responsible for the checkpoint control of cell cycles (42,43). Natural compounds acting as cell cycle arrest agents can disrupt cell cycle progression (44). Hence, the effect of ECa 233 on cell cycle progression was also explored. In the present study, we found that treatment of KON cells with ECa 233 resulted in cell cycle arrest in the G0/G1 phase, suggesting that the chemical constituents of ECa 233 mediated this activity. The KON cells in the G1, S, and G2-M phases after exposure to the high concentrations of ECa 233 were dramatically decreased. It is possible that ECa 233 could modulate cell cycle regulators' expression, which had a predominant role in controlling the cell cycle and induced cells to undergo apoptosis as well as exit from the cell cycle. Moreover, the molecular mechanism to modulate cell cycle progression was thoroughly investigated to describe its action.

The colony formation assay is a gold standard *in vitro* experiment tool based on the ability of a single cell to proliferate and grow into a large colony that determines cell reproductivity after treatment with ECa 233 (45-47). The results demonstrated that ECa 233 significantly repressed the ability of KON cells to proliferate into large colonies and suggest that ECa 233 effectively inhibited KON cells from producing a viable colony after treatment for 24 h, regardless of one mechanism, as long as the ECa 233 affects the cells' reproductive ability to form progenies. Cancer migration and invasion are constitutive components of metastatic disease, which is the crucial cause of mortality/lethality in cancer patients. The primary step of the metastatic cascade is invasion, which allows cancer cells to penetrate the surrounding tissue and basement membrane and to migrate through the extracellular matrix into the surrounding tissue, a process that is promoted by tumor microenvironments (48,49). The present data demonstrated that ECa 233 significantly reduced the migratory ability of KON cells and promoted wound healing in a concentration-dependent manner. The present study did not identify the mechanisms underlying the anti-migratory effects of ECa 233, which need to be further investigated to describe their action. The ability of cell migration and invasion was checked in the KON cells after ECa 233 exposure through the transwell migration/Matrigel invasion assay. The results of the present study indicate that migrative and invasive capacity was limited by ECa 233 in a concentration-reliant manner, suggesting that ECa 233 has the potential to abrogate the movement and invasion behavior of KON cells. These results support the use of ECa 233 as an anti-migratory and anti-invasive agent as well as for the development of a suitable formulation to target inside cancer cells and provide an appropriate pharmaceutical product applicable for oral cancer patients.

Previous studies also revealed that asiaticoside, one component of ECa 233, inhibited the cell growth of the drug-resistant myeloma cell line KM3/BTZ and inhibited migratory and invasive properties by modulation of the STAT-3 signaling pathway, indicating its potential (50). In another study, it was shown that asiaticoside inhibited the ionizing radiation-induced migration and invasion of A549 human lung cancer cells at noncytotoxic concentrations, leading to reduced local recurrence or distant metastasis beneficial radiotherapy in patients with non-small-cell lung cancer (51). Other previous research demonstrated that ERα expression is a prognostic marker and therapeutic target and indicated that a rare expression of ERα in a large patient cohort study was associated with a dramatic decrease in overall survival in male patients (52). Another study revealed the ER-mediated signaling pivotal role in oral cancer progression by supporting the proliferation, invasion, and chemoresistance of OSCC cells, preferring its dominance for designing drug treatment to eliminate the signaling (53). Regarding the results in the E_2-induced cell migration and invasion condition, ECa 233 could modulate the effects of E_2-induced migratory and invasion drivers in KON cells in a dose-dependent fashion. It may be possible that the expression of ERs inside KON cells acts as a new receptor for dissecting the E_2 signaling pathways. Therefore, E_2 may act as a growth factor or crucial factor in the induced cell migration and invasion capacity of KON cells. It may represent the ERs inside the KON cells, which is a supportive hallmark of cancer cells, and may be applied as a new therapeutic targeting to dissect the residue of E_2 signaling pathways that induce cell proliferation. However, the representative of the ERs inside KON cells should be further studied to describe the detailed mechanism underlying E_2-induced cell growth. In addition, ECa 233 can penetrate inside the KON cells by affecting the cell structure and cell stability. Multicellular tumor spheroids are three-dimensional structures composed of the aggregation of KON cells in a round bottom 96-well plate, mimicking the *in vivo* architecture of natural organs and tissues (54,55). Any natural active constituent that provides the inhibition of spheroid formation would be a prospect for an anti-tumor drug. This is the reason for investigating anti-spheroid formation. The results demonstrated that ECa 233 effectively repressed the size of the multicellular spheroids of KON cells after being treated with ECa 233 for 24 h and that ECa 233 may modulate the large formation of KON cells, which leads to decreasing colonization. It is possible that ECa 233 blocks the cell-cell/cell-matrix interactions and function of spheroids. ECa 233 also showed good ADMET properties. However, the absorption value of madecassoside and asiaticoside is less than 30%. Therefore, a new formulation to modify the absorption value or engineered drug delivery system to improve the poor solubility issue is a particularly urgent need as well as successfully controlled drug release and higher oral bioavailability delivery. Furthermore, advanced technology needs to be developed for the successful delivery of drugs to the target sites in oral cancer cells. Previous studies provided pharmacokinetic and metabolomic data of an orally modified formulation of standardized *Centella asiatica* extract in healthy volunteers, which showed that the major component compounds, madecassoside and asiaticoside, are poorly absorbed, and instead underwent the biotransformation into active metabolites with minimal renal excretion. The active metabolites of madecassoside and asiaticoside are highly lipophilic molecules and are possibly eliminated through the hepatobiliary system and then mostly excreted through the fecal route (56). ECa 233 is a plant-derived compound that has tremendous pharmacological applications. Further studies are required to evaluate and confirm the pharmacological effects and application of ECa 233 both *in vitro* and *in vivo* experiments.

CONCLUSIONS

In summary, ECa 233 provided antiproliferative effects against KON cells by inducing the apoptosis associated with ROS generation and acting as a G0/G1 cell cycle arrest agent. ECa 233 modulated the habitual

hallmarks of KON cells by affecting the migratory/invasive ability as well as the stability and cell structure of the KON cells. Thus, the pharmacokinetics of ECa 233 are of interest and offer solid groundwork for further investigation in the future. Moreover, ECa 233 may be considered an excellent source of highly effective phytochemicals for oral cancer therapy.

Acknowledgments

The authors received no grant support or external funding for this research. The authors would like to thank the Faculty of Pharmaceutical Sciences, Burapha University for providing the laboratory facilities and equipment.

Conflict of interest statement

The authors declared no conflict of interest in this study.

Authors' contributions

S. Manmuan contributed to the conceptualization, methodology, data curation, formal analysis, validation, and the writing of the original draft of the article; S. Manmuan and S. Tubtimsri were responsible for the resources and investigation; S. Manmuan, S. Tubtimsri, N. Chaothanaphat, N. Issaro, and P. Manmuan performed the review and editing of the manuscript; S. Tubtimsri, N. Issaro, and M.H. Tantisira were responsible for the visualization and suggestions. The finalized article was read and approved by all authors.

REFERENCES

1. Charly MM, Jean-Paul SI, Ngbolua KTN, Hippolyte SNT, Erick KN, Alifi PB, *et al*. Review of the literature on oral cancer: epidemiology, management and evidence-based traditional medicine treatment. Annu Res Rev Biol. 2022;37(6):15-27. DOI: 10.9734/arrb/2022/v37i630512.
2. Kumar M, Nanavati R, Modi T, Dobariya C. Oral cancer: etiology and risk factors: a review. J Cancer Res Ther. 2016;12(2):458-463. DOI: 10.4103/0973-1482.186696.
3. Warnakulasuriya S, Kerr AR. Oral cancer screening: past, present, and future. J Dent Res. 2021;100(12):1313-1320. DOI: 10.1177/00220345211014795.
4. Rivera C. Essentials of oral cancer. Int J Clin Exp Pathol. 2015;8(9):11884-11894. PMCID: PMC4637760.
5. Cristaldi M, Mauceri R, Di Fede O, Giuliana G, Campisi G, Panzarella V. Salivary biomarkers for oral squamous cell carcinoma diagnosis and follow-up: current status and perspectives. Front Physiol. 2019;10:1476,1-12. DOI: 10.3389/fphys.2019.01476.
6. Mascitti M, Orsini G, Tosco V, Monterubbianesi R, Balercia A, Putignano A, *et al*. An overview on current non-invasive diagnostic devices in oral oncology. Front Physiol. 2018;9:1510,1-8. DOI: 10.3389/fphys.2018.01510.
7. Sha J, Bai Y, Ngo H, Okui T, Kanno T. Overview of evidence-based chemotherapy for oral cancer: focus on drug resistance related to the epithelial-mesenchymal transition. Biomolecules. 2021;11(6):893,1-23. DOI: 10.3390/biom11060893.
8. Zhang M, Liang J, Yang Y, Liang H, Jia H, Li D. Current trends of targeted drug delivery for oral cancer therapy. Front Bioeng Biotechnol. 2020;8:618931,1-11. DOI: 10.3389/fbioe.2020.618931.
9. Kinghorn AD, Chin YW, Swanson SM. Discovery of natural product anticancer agents from biodiverse organisms. Curr Opin Drug Discov Devel. 2009;12(2):189-196. PMCID: PMC2877274.
10. Huang M, Lu JJ, Ding J. Natural products in cancer therapy: past, present and future. Nat Prod Bioprospect. 2021;11(1):5-13. DOI: 10.1007/s13659-020-00293-7.
11. Ferreira AS, Macedo C, Silva AM, Delerue-Matos C, Costa P, Rodrigues F. Natural products for the prevention and treatment of oral mucositis-a review. Int J Mol Sci. 2022;23(8):4385,1-31. DOI: 10.3390/ijms23084385.
12. Osborne CK, Schiff R. Estrogen-receptor biology: continuing progress and therapeutic implications. J Clin Oncol. 2005;23(8):1616-1622. DOI: 10.1200/JCO.2005.10.036.
13. Thomas C, Gustafsson JA. The different roles of ER subtypes in cancer biology and therapy. Nat Rev Cancer. 2011;11(8):597-608. DOI: 10.1038/nrc3093.
14. Altwegg KA, Vadlamudi RK. Role of estrogen receptor coregulators in endocrine resistant breast cancer. Explor Target Antitumor Ther. 2021;2:385-400. DOI: 10.37349/etat.2021.00052.
15. Ishida H, Wada K, Masuda T, Okura M, Kohama K, Sano Y, *et al*. Critical role of estrogen receptor on anoikis and invasion of squamous cell carcinoma. Cancer Sci. 2007;98(5):636-643. DOI: 10.1111/j.1349-7006.2007.00437.x.
16. Kim MJ, Lee JH, Kim YK, Myoung H, Yun PY. The role of tamoxifen in combination with cisplatin on oral squamous cell carcinoma cell lines. Cancer Lett. 2007;245(1-2):284-292. DOI: 10.1016/j.canlet.2006.01.017.
17. Egloff AM, Rothstein ME, Seethala R, Siegfried JM, Grandis JR, Stabile LP. Cross-talk between estrogen

receptor and epidermal growth factor receptor in head and neck squamous cell carcinoma. Clin Cancer Res. 2009;15(21):6529-6540.
DOI: 10.1158/1078-0432.09-0862.

18. Chang YL, Hsu YK, Wu TF, Huang CM, Liou LY, Chiu YW, *et al*. Regulation of estrogen receptor alpha function in oral squamous cell carcinoma cells by FAK signaling. Endocr Relat Cancer. 2014;21(4):555-565.
DOI: 10.1530/ERC-14-0102.
19. Hussin F, Eshkoor SA, Rahmat A, Othman F, Akim A. The *Centella asiatica* juice effects on DNA damage, apoptosis and gene expression in hepatocellular carcinoma (HCC). BMC Complement Altern Med. 2014;14:32,1-7.
DOI: 10.1186/1472-6882-14-32.
20. Rotpenpian N, Arayapisit T, Roumwong A, Pakaprot N, Tantisira M, Wanasuntronwong A. A standardized extract of *Centella asiatica* (ECa 233) prevents temporomandibular joint osteoarthritis by modulating the expression of local inflammatory mediators in mice. J Appl Oral Sci. 2021;29:e20210329, 1-8.
DOI: 10.1590/1678-7757-2021-0329.
21. Teerapattarakan N, Benya-Aphikul H, Tansawat R, Wanakhachornkrai O, Tantisira MH, Rodsiri R. Neuroprotective effect of a standardized extract of *Centella asiatica* ECa233 in rotenone-induced parkinsonism rats. Phytomedicine. 2018;15(44): 65-73.
DOI: 10.1016/j.phymed.2018.04.028.
22. Pittella F, Dutra RC, Junior DD, Lopes MT, Barbosa NR. Antioxidant and cytotoxic activities of *Centella asiatica* (L) Urb. Int J Mol Sci. 2009;10(9): 3713-3721.
DOI: 10.3390/ijms10093713.
23. Wanasuntronwong A, Tantisira MH, Tantisira B, Watanabe H. Anxiolytic effects of standardized extract of *Centella asiatica* (ECa 233) after chronic immobilization stress in mice. J Ethnopharmacol. 2012;143(2):579-585.
DOI: 10.1016/j.jep.2012.07.010.
24. Wanasuntronwong A, Wanakhachornkrai O, Phongphanphanee P, Isa T, Tantisira B, Tantisira MH. Modulation of neuronal activity on intercalated neurons of amygdala might underlie anxiolytic activity of a standardized extract of *Centella asiatica* ECa233. Evid Based Complement Alternat Med. 2018;2018:3853147,1-8.
DOI: 10.1155/2018/3853147.
25. Boondam Y, Songvut P, Tantisira MH, Tapechum S, Tilokskulchai K, Pakaprot N. Inverted U-shaped response of a standardized extract of *Centella asiatica* (ECa 233) on memory enhancement. Sci Rep. 2019;9(1):8404:1-11.
DOI: 10.1038/s41598-019-44867-z.
26. Boondam Y, Tantisira MH, Tilokskulchai K, Tapechum S, Pakaprot N. Acute enhancing effect of a standardized extract of *Centella asiatica* (ECa 233) on synaptic plasticity: an investigation *via* hippocampal long-term potentiation. Pharm Biol. 2021;59(1):365-372.
DOI: 10.1080/13880209.2021.1893348.
27. Moolsap F, Tanasawet S, Tantisira MH, Hutamekalin P, Tipmanee V, Sukketsiri W. Standardized extract of *Centella asiatica* ECa 233 inhibits lipopolysaccharide-induced cytokine release in skin keratinocytes by suppressing ERK1/2 pathways. Asian Pac J Trop Biomed. 2020;10(6):273-280.
DOI: 10.4103/2221-1691.283941.
28. Anukunwithaya T, Tantisira MH, Shimada T, Sai Y, Khemawoot P. Multiple oral dosing pharmacokinetics of standardized extract of *Centella asiatica* ECa 233 and its inductive effect on efflux transporters in rats. Planta Med Int Open. 2017;4:e66-e73.
DOI: 10.1055/s-0043-114669.
29. Anukunwithaya T, Tantisira MH, Tantisira B, Khemawoot P. Pharmacokinetics of a standardized extract of *Centella asiatica* ECa 233 in rats. Planta Med. 2017;83(8):710-717.
DOI: 10.1055/s-0042-122344.
30. Wang S, Yang M, Li R, Bai J. Current advances in noninvasive methods for the diagnosis of oral squamous cell carcinoma: a review. Eur J Med Res. 2023;28(53):1-13.
DOI: 10.1186/s40001-022-00916-4.
31. Liu SA, Tsai WC, Wong YK, Lin JC, Poon CK, Chao SY, *et al*, *et al*. Nutritional factors and survival of patients with oral cancer. Head Neck. 2006;28(11):998-1007.
DOI: 10.1002/hed.20461.
32. Gonzalez-Moles MA, Aguilar-Ruiz M, Ramos-Garcia P. Challenges in the early diagnosis of oral cancer, evidence gaps and strategies for improvement: a scoping review of systematic reviews. Cancers. 2022;14(19):4967,1-30.
DOI: 10.3390/cancers14194967.
33. Varela-Centelles P. Early diagnosis and diagnostic delay in oral cancer. Cancers. 2022;14(7):1758,1-3.
DOI: 10.3390/cancers14071758.
34. Huang M, Lu JJ, Ding J. Natural products in cancer therapy: past, present and future. Nat Prod Bioprospect.2021;11(1):5-13.
DOI: 10.1007/s13659-020-00293-7.
35. Hashem S, Ali TA, Akhtar S, Nisar S, Sageena G, Ali S, *et al*. Targeting cancer signaling pathways by natural products: exploring promising anti-cancer agents. Biomed Pharmacother. 2022;150:113054,1-12.
DOI: 10.1016/j.biopha.2022.113054.
36. Orhan IE. *Centella Asiatica* (l.) urban: from traditional medicine to modern medicine with neuroprotective potential. Evid Based Complementary Altern Med. 2012;2012:946259,1-8
DOI: 10.1155/2012/946259.
37. Sukketsiri W, Tanasawet S, Moolsap F, Tantisira MH, Hutamekalin P, Tipmanee V. ECa 233 suppresses LPS-induced proinflammatory responses in macrophages via suppressing ERK1/2, p38 MAPK and Akt pathways. Biol Pharm Bull. 2019;42(8):1358-1365.
DOI: 10.1248/bpb.b19-00248.

38. Songvut P, Chariyavilaskul P, Tantisira MH, Khemawoot P. Safety and pharmacokinetics of standardized extract of *Centella asiatica* (ECa 233) capsules in healthy Thai volunteers: a phase 1 clinical study. Planta Med. 2019;85(6):483-490. DOI: 10.1055/a-0835-6671.
39. Manmuan S, Manmuan P, Yoykaew P, Thuetong P, Asipong P, Riantong N, *et al*. Evaluation of standardized extract of *Centella asiatica* on cell viability and repressive cancer migration in metastatic colorectal cancer cells *in vitro*. Walailak J Scie. 2021;18(5):1-18. DOI: 10.48048/wjst.2021.9016.
40. Singh V, Khurana A, Navik U, Allawadhi P, Bharani KK, Weiskirchen R. Apoptosis and pharmacological therapies for targeting thereof for cancer therapeutics. Sci. 2022;4,15:1-25. DOI: 10.3390/sci4020015.
41. Fitzgerald MC, O'Halloran PJ, Connolly NMC, Murphy BM. Targeting the apoptosis pathway to treat tumours of the paediatric nervous system. Cell Death Dis. 2022;13(5),460:1-12. DOI: 10.1038/s41419-022-04900-y.
42. Hanahan D, Weinberg RA Hallmarks of cancer: the next generation. Cell. 2011;144(5):646-674. DOI: 10.1016/j.cell.2011.02.013.
43. Chantree P, Na-Bangchang K, Martviset P. Anticancer activity of fucoidan *via* apoptosis and cell cycle arrest on cholangiocarcinoma cell. Asian Pac J Cancer Prev. 2021;22(1):209-217. DOI: 10.31557/APJCP.2021.22.1.209.
44. Bailon-Moscoso N, Cevallos-Solorzano G, Romero-Benavides JC, Orellana MI. Natural compounds as modulators of cell cycle arrest: application for anticancer chemotherapies. Curr Genomics. 2017;18(2):106-131. DOI: 10.2174/1389202917666160808125645.
45. Franken NA, Rodermond HM, Stap J, Haveman J, van Bree C. Clonogenic assay of cells *in vitro*. Nat Protoc. 2006;1(5):2315-2319. DOI: 10.1038/nprot.2006.339.
46. Katz D, Ito E, Lau KS, Mocanu JD, Bastianutto C, Schimmer AD, *et al*. Increased efficiency for performing colony formation assays in 96-well plates: novel applications to combination therapies and high-throughput screening. Biotechniques. 2018;44(2):ix-xiv,1-6. DOI: 10.2144/000112757.
47. Braselmann H, Michna A, Hess J, Unger K. CFAssay: statistical analysis of the colony formation assay. Radiat Oncol J. 2015;10:223,1-6. DOI: 10.1186/s13014-015-0529-y.
48. Novikov NM, Zolotaryova SY, Gautreau AM, Denisov EV. Mutational drivers of cancer cell migration and invasion. Br J Cancer. 2021;124(1):102-114. DOI: 10.1038/s41416-020-01149-0.
49. Wu JS, Jiang J, Chen BJ, Wang K, Tang YL, Liang XH. Plasticity of cancer cell invasion: patterns and mechanisms. Transl Oncol. 2021;14(1):100899,1-9. DOI: 10.1016/j.tranon.2020.100899.
50. Yingchun L, Huihan W, Rong Z, Guojun Z, Ying Y, Zhuogang L. Antitumor activity of asiaticoside against multiple myeloma drug-resistant cancer cells is mediated by autophagy induction, activation of effector caspases, and inhibition of cell migration, invasion, and STAT-3 signaling pathway. Med Sci Monit. 2019;25:1355-1361. DOI: 10.12659/MSM.913397.
51. Han AR, Lee S, Han S, Lee YJ, Kim JB, Seo EK, *et al*. Triterpenoids from the leaves of *Centella asiatica* inhibit ionizing radiation-induced migration and invasion of human lung cancer cells. Evid Based Complementary Altern Med. 2020;2020: 3683460,1-7. DOI: 10.1155/2020/3683460.
52. Doll C, Bestendonk C, Kreutzer K, Neumann K, Pohrt A, Trzpis I, *et al*. Prognostic significance of estrogen receptor alpha in oral squamous cell carcinoma. Cancers. 2021;13(22):5763,1-13. DOI: 10.3390/cancers13225763.
53. Takei RA, Tomihara K, Yamazaki M, Moniruzzaman R, Heshiki W, Sekido K, *et al*. Protumor role of estrogen receptor expression in oral squamous cell carcinoma cells. Oral Surg Oral Med Oral Pathol Oral Radiol. 2021;132(5):549-565. DOI: 10.1016/j.oooo.2021.04.006.
54. Achilli TM, Meyer J, Morgan JR. Advances in the formation, use and understanding of multi-cellular spheroids. Expert Opin Biol Ther. 2012;12(10):1347-1360. DOI: 10.1517/14712598.2012.707181.
55. Cui X, Hartanto Y, Zhang H. Advances in multicellular spheroids formation. J R Soc Interface. 2017;14(127),20160877:1-15. DOI: 10.1098/rsif.2016.0877.
56. Songvut P, Chariyavilaskul P, Khemawoot P, Tansawat R. Pharmacokinetics and metabolomics investigation of an orally modified formula of standardized *Centella Asiatica* extract in healthy volunteers. Sci Rep. 2021;11(1):6850,1-13. DOI: 10.1038/s41598-021-86267-2.